Winter 1996

Modelling an Optical Fiber Bragg Grating

Claudio Oliveira Egalon
Old Dominion University

MODELLING AN OPTICAL FIBER BRAGG GRATING

by

Claudio Oliveira Egalon

B.Sc. in Physics, December 1984, Federal University of Rio de Janeiro, Brazil
M.Sc. in Physics, The College of William and Mary, December 1988
Ph.D. in Physics, The College of William and Mary, May 1990

A Dissertation submitted to the Faculty of
Old Dominion University in Partial Fulfillment of the
Requirement for the Degree of

DOCTOR OF PHILOSOPHY

ELECTRICAL ENGINEERING

OLD DOMINION UNIVERSITY
December 1996

Approved by:

_____
Dr. Sacharia Albin

_____
Dr. Linda L. Vahala

_____
Dr. Vishnu K. Lakdawala

_____
Dr. John B. Cooper

ABSTRACT

MODELLING AN OPTICAL FIBER BRAGG GRATING

Claudio Oliveira Egalon

Old Dominion University, 1996

Director: Dr. Sacharia Albin

A theoretical investigation of a single mode optical fiber with one and two superimposed Bragg grating is presented. The formulation relies in the determination of an approximate solution in the asymptotic region of one of the fiber parameters. A correction is then applied to the asymptotic solution using the Method of the Successive Approximations also known as the Piccard Method. The approximation was then compared to the numerical solution using the Runge-Kutta method. Assuming that each Bragg grating has modulation frequencies given by Ω_1 and Ω_2, it has been found that the second Bragg grating shifts the peak reflectivity of the first one by a small amount. The direction of the shift depends on the relative value of Ω_1 and Ω_2. The fiber Bragg grating solution has been succesfully applied to other fiber devices.

AKNOWLEDGEMENTS

I would like to express my appreciation to Dr. Sacharia Albin, from ODU, for his guidance during the course of this research. His hard work and tolerance helped me accomplished several major milestones throughout these four years of graduate study. Unvaluable support was provided by Dr. Robert S. Rogowski and Mr. Leland Melvin from NASA Langley Research Center. They provided insightful discussions that led to the definition of the problem presented here. I am also in debt to Dr. A. Martin Buoncristiani, from Christopher Newport University, for providing his time to discuss several aspects of this problem. He and Mr. Arnel Lavarias, a colleague from ODU, provided independent confirmation of the correctness of the numerical solution of two co-propagating modes generated by myself. These independent confirmations gave me assurances that a previous result published in the literature was not correct. Finally, my thanks go to the remaining members of the commitee Dr. Linda Vahala, Dr. Vishnu Lakdawala and Dr. John Cooper for reviewing the dissertation and providing comments before, during and after the oral defense.

TABLE OF CONTENTS

Page

AKNOWLEDGEMENTS iii

TABLE OF CONTENTS iv

LIST OF TABLES vii

LIST OF FIGURES viii

CHAPTERS

I. INTRODUCTION 1

1. Historical Background 1

2. Research Overview 4

II. THE COUPLED MODE EQUATIONS 6

1. Introduction 6

2. Outline of the derivation of the coupled mode equations 8

III. OPTICAL FIBER BRAGG GRATINGS 14
1. Introduction 14
2. Advances in Fabrication Techniques 15
3. Characteristics 17
4. Devices 20
1. Optical fiber lasers 20
2. Optical fiber filters and mode converters 21
3. Optical fiber sensors 23
5. Summary 24

IV. COUPLED EQUATIONS OF AN OPTICAL FIBER WITH A SINGLE BRAGG GRATING 25
1. Introduction 25
2. The Asymptotic Solution 27
3. Comparison between asymptotic and numerical solutions 30
4. Reflectivity of a single mode fiber with a single Bragg grating 35
5. Summary 37

V. COUPLED EQUATIONS OF AN OPTICAL FIBER WITH DUAL BRAGG GRATINGS 38
1. Introduction 38
2. The modified asymptotic solution 40
3. Comparison between approximate and numerical solutions 44
4. Estimate of the shift in wavelength due to a second Bragg grating 52

VI. APPLICATIONS OF THE OPTICAL FIBER BRAGG
GRATING SOLUTION TO OTHER DEVICES 54
1. Introduction 54
2. Coupled Equations for a two Mode Fiber 54
3. Conditions for Coupling Among Modes in a Four Mode Fiber 57
4. Effects of Temperature and Axial Strain in the Bragg Wavelength 60

VII. CONCLUSIONS 67

LIST OF REFERENCES 69

APPENDICES 75
A. Derivation of the First Order Correction 75
B. Interval of Convergence of the First Order Approximation 78
C. Typical Values of the Fiber Parameters 82
D. Solution of the Coupled Equations for two Co-Propagating Modes 86

VITA 95

LIST OF TABLES

Table *Page*

1. Optical fiber dopants for optical fiber lasers 19

2. Slope values for the shift of the Bragg wavelength at 1300 and 850 n*m*, for mechanical and thermal strain. Experimental values are from Xu et al. [1994] whereas theoretical values are from Equations (73) and (75). Parameters used are for a silica fiber. 66

LIST OF FIGURES

Figure *Page*

1. Mode coupling in a translationally variant fiber..... 7

2. A semi-infinite uniform fiber excites only forward propagating modes..... 11

3. The end-face of a finite uniform fiber can introduce backward propagating modes through Fresnel reflections 11

4. A second light source at the other endface of the fiber can introduce backward propagating modes in the fiber..... 13

5. Experimental set-up used by Hill et al. [1978] to write a Bragg grating..... 15

6. Experimental set-up for external writing [Meltz et al., 1989]..... 16

7. Reflection spectrum of a single Bragg grating at wavelength 1.3 μm. The normalized coupling constant was assumed to be 2.0,for n_{core}=1.46 and L=0.03 m 22

8. Experimental set-up for a mode converter..... 23

9. Numerical and asymptotic solutions for the transferred power against the normalized position 33

Figure *Page*

10. Numerical (dashed curves) and asymptotic (solid curves) solutions for the transferred power against the normalized position in an optical fiber Bragg grating nearby the phase matching condition, γ=0. The higher the value of the coupling constant, the more the numerical and approximate solutions deviates from each other 34

11. Contour plot of the Reflectivity against the normalized coupling constant and the normalized phase matching parameter for a single Bragg grating optical fiber. At a given value of the coupling constant, the reflectivity is maximum at γ=0 36

12. Comparison between numerical (dashed lines) and approximate (solid lines) solutions for an optical fiber with two co-located Bragg gratings (α_1=100,000, α_2=99,950, γ_1=0, γ_2=50 and C_{00}=0.1, C_{00}=5 and C_{00}=7)..... 45

13. Comparison between numerical (dashed lines) and approximate (solid lines) solutions for an optical fiber with two co-located Bragg gratings (α_1=100,000, α_2=99,950, γ_1=0, γ_2=10 and C_{00}=0.1, C_{00}=5 and C_{00}=7)..... 46

14. Comparison between numerical (dashed lines) and approximate (solid lines) solutions for an optical fiber with two co-located Bragg gratings (α_1=100,000, α_2=99,950, γ_1=1, γ_2=10 and C_{00}=0.5, C_{00}=1.1 and C_{00}=2)..... 47

Figure *Page*

15. Contour plot of the reflectivity against the two normalized phase matching parameters of a dual Bragg grating optical fiber for $C_{00}=1$ ($\gamma_2>0$)..... 49

16. Contour plot of the reflectivity against the two normalized phase matching parameters of a dual Bragg grating optical fiber for $C_{00}=1$ ($\gamma_2<0$)..... 50

17. Optical fiber with a blazed Bragg grating..... 57

18. Contour plot of the normalized coupling constant against the V-number and the amplitude modulation of the refractive index for $L=0.01m$, $n_{core}=1.46$, $a=5.0\ \mu m$, $\Delta=0.01$ 83

19. Plot of the α parameter against the V-number for $L=0.01m$, $n_{core}=1.46$, $a=5.0\ \mu m$, $\Delta=0.01$ 85

20. Comparison between the asymptotic, first order and numerical solutions for the transferred power against the normalized length of two co-propagating modes ($\alpha'=2\gamma'$, $\gamma'=5$) 88

21. Comparison between the asymptotic, numerical and first order solutions of Snyder and Davis [1970] for the transferred power against the normalized length of two co-propagating modes ($\alpha'=2\gamma'$, $\gamma'=5$) 90

Figure *Page*

22. Comparison between the asymptotic, first order and numerical solutions for the transferred power against the normalized length of two co-propagating modes ($\alpha'=2\gamma'$, $\gamma'=2.5$) 91

23. Comparison between the asymptotic, numerical and first order solutions of Snyder and Davis [1970] for the transferred power against the normalized length of two co-propagating modes ($\alpha'=2\gamma'$, $\gamma'=5$) 92

CHAPTER I

INTRODUCTION

I.1 Historical Background

The coupled mode equations can be used to solve several important problems in Physics and Engineering [Cardimona et al., 1995; Shi and Okoshi, 1992a and b; Huang et al., 1992; Haus and Huang, 1991; Marcuse, 1990; Lam and Garside, 1981; Yariv, 1989; Park et al., 1989 and Kogelnik and Shank, 1972]. They have been used to model distributed feedback (DFB) lasers, [Kogelnik and Shank, 1972; Yariv 1989 and Marcuse, 1990], intermodal switches and mode converters [Park and et al., 1989; Bilodeau et al., 1991 and Shi and Okoshi 1992a and b], optical fiber filters [Hill et al., 1978 and Lam and Garside, 1981], optical fiber sensors [Morey et al., 1989 and 1994] and other devices.

Kogelnik and Shank [1972] have analyzed the laser action in a periodic structure using the coupled mode equations. This procedure has been repeated by Yariv [1989] to determine the longitudinal modes of vibration of a laser whereas Marcuse [1990] presented a theoretical study of a DFB laser with an attached external intensity modulator.

Mode converters have been fabricated by Hill et al. [1990] and Bilodeau et al. [1991]. These converters use a periodic grating to transfer power from the

fundamental to higher order modes and have applications in bimodal networks [Blake et al., 1986 and Park and Kim, 1989]. Shi and Okoshi [1992] undertook a theoretical analysis of one of these converters, the $LP_{01} \leftrightarrow LP_{02}$ converter, and determined that a narrow spectrum of power conversion could be obtained by reducing the index perturbation, the core-cladding refractive index difference and the core radius.

Hill et al., [1978] were the first to propose that a reflection filter could be fabricated from a photosensitive optical fiber. Additional work by Lam and Garside [1981] demonstrated that the solution of the coupled mode equations of an optical fiber with a periodic grating compared very well with experiments they have undertaken. They found, among other results, that the spectral bandwidth increases with the writing power of the laser.

Finally, the coupled mode equations have been used to determine the behaviour of optical fiber sensors for strain and temperature [Morey et al., 1989 and 1994]. These sensors use the shift in the Bragg wavelength to determine the parameters to be measured.

This work is concerned with the solution of the coupled mode equations applied to optical fiber Bragg gratings. An exact analytical solution for this kind of equation is not known but it is possible to obtain an approximate solution in the asymptotic region of one of its parameters [Miller, 1968; Snyder and Davis, 1970; Kogelnik and Shank, 1972; Lam and Garside,1981; Snyder and Love, 1983; Haus and Huang, 1991 and Shi and Okoshi, 1992a]. This asymptotic solution, although not exact, fits very well the experimental

results [Limberger et al., 1993] because of the order of magnitude of the wavelength of the light and the period of its associated Bragg grating. These quantities make up the so-called α-parameter that is used in the asymptotic region, i.e., $\alpha \Rightarrow \infty$. However, if α were to be lower, the asymptotic solution would not work as well and a first order correction would be required.

Although this asymptotic solution has been known for some time [Miller, 1968; Snyder and Davis, 1970; Kogelnik and Shank, 1972; Lam and Garside,1981; Snyder and Love, 1983; Haus and Huang, 1991 and Shi and Okoshi, 1992a], a clear detailed mathematical procedure outlining its derivation has not been found. The derivations found in the literature restrict to qualitative explanations such as neglecting the high frequency terms of the coupled mode equations [Yariv, 1989 and Snyder and Love, 1983] but present no transparent straight-forward mathematical procedure that justifies this assumption. Maybe, the best attempt at its derivation was made by Snyder and Davis [1970]. However, it has been found that the procedure presented is not self-consistent and their first order correction does not agree with the numerical solution [see Appendix D and Egalon et al., 1996]. Furthermore, extensive comparison between the asymptotic and numerical solutions has not been found in the literature as well.

I.2 Research Overview

In this work, a clear, straight-forward mathematical procedure is outlined in the derivation of the asymptotic solution of a single mode optical fiber with a single Bragg grating. This solution was then used to determine a first order correction to the asymptotic solution which may apply whenever a second, co-located, Bragg grating is super-imposed to the first one. This procedure can be used to determine the effects of additional gratings, blazed gratings, multimode optical fibers, tapered couplers etc. The method presented here is a modified and improved version of the procedure outlined by Snyder and Davis [1970] which was found to make unnecessary assumptions and to be slightly inconsistent [Appendix D and Egalon et al., 1996]. For this reason, some of this formulation had to be modified leading to an improved version. Basically, the method consists of

i) determining an approximate solution of the coupled mode equations using an asymptotic assumption and
ii) applying a first order correction to the asymptotic solution using the Method of the Successive Approximations, also known as the Piccard Method [Ince, 1956; Greenspan, 1960; Rowe, 1962 and Volpert and Volpert, 1990].

These approximate solutions were then compared to a numerical solution obtained by using the Runge Kutta method. Since the coupled mode equations of a single mode fiber is basically a Boundary Value problem, an initial guess, or initial value, had to be provided to the numerical solution. This initial value was chosen from the approximate solution derived, and the

final numerical result compared to the analytical formulas throughout the domain of values.

For the case of two superimposed Bragg gratings it was found that the second grating produces a very small shift in the wavelength of the peak reflectivity of the first grating; the very presence of this term can shift this wavelength either towards longer or shorter values. However, it has also been found that this correction can be neglected at least for the range of parameters used.

Although an exact solution for the coupled mode equations with a periodic variation in the refractive index along the propagation length of the wave is not known, there is sufficient evidence in the literature that shows that an approximate solution can be applied to many optical devices. Several of them, such as DFB lasers, mode converters, optical fiber reflection filters and sensors have been analysed using this approximate solution leading to results that are compatible with experiments.

CHAPTER II

THE COUPLED MODE EQUATIONS

II.1 Introduction

It is a well known theoretical result that transference of power among modes does not occur in translationally invariant fibers [Marcuse, 1974 and Snyder and Love, 1983]. In this kind of fibers, the refractive index profile, n, and the core radius, a, are invariant along its length, i.e., they are independent of the axial coordinate z. However, if a fiber is translationally *variant*, mode coupling, or transference of power among modes, will occur. This coupling can be explained by the fact that the V-number –a parameter that determines the number of modes in a fiber–, varies along the fiber length. Because the fraction of power in a given mode of an optical fiber is a function of the V-number, it is reasonable to assume that a rearrangement of power among the modes in a fiber takes place once the V-number varies along its length. In other words variations in the V-number causes the power in a given mode to change. Since the total power must be conserved, any difference must be transferred to other modes.

This coupling can occur among bound and/or radiation modes and it can be described as a set of coupled differential equations [Marcuse, 1973 and 1974; Yariv, 1989 and Snyder and Love, 1983]. For instance, assuming that the power transferred among bound and radiation modes can be ignored in a

single mode fiber, coupling will take place only between the forward and backward propagating fundamental modes (see Fig. 1). In this case, the coupling is essentially a reflection, a transference of power towards the backward propagating mode.

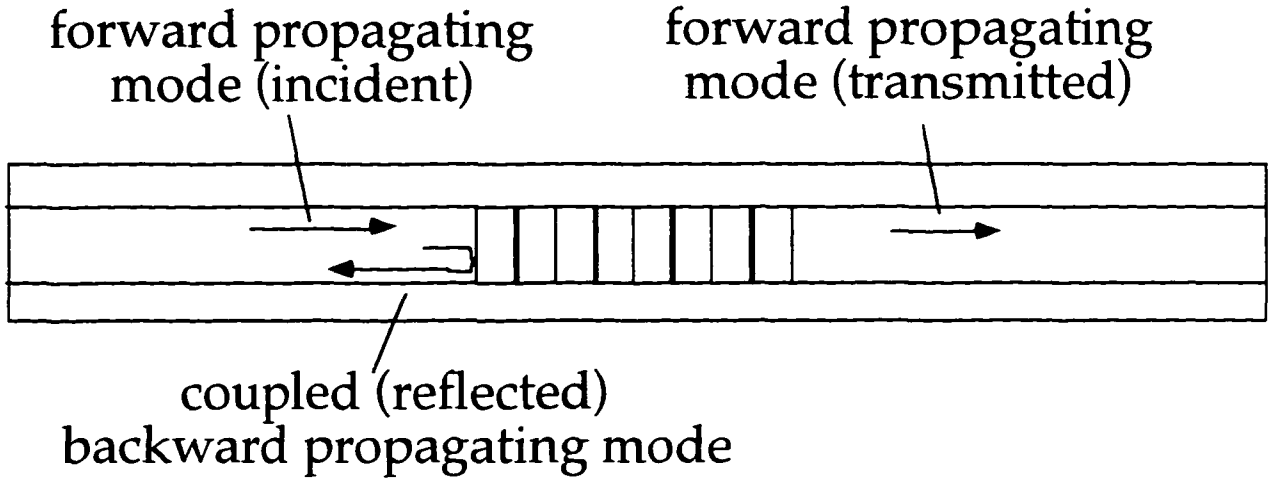

Figure 1. Mode coupling in a translationally variant fiber

Similarly, in the case of a two mode fiber, coupling may take place among the forward and backward propagating LP_{01} and LP_{11} modes. However, in the particular case where an optical fiber has a Bragg grating perpendicular to the fiber axis, no coupling occurs between these modes. This happens because the coupling constants between them, k_{01} and k_{10}, are zero, whereas the coupling constants between the forward and backward fundamental modes, k_{00}, and the forward and backward LP_{11} modes, k_{11}, are different from zero (see Chapter VII). Chapter VII also shows that, for coupling between the LP_{01} and LP_{11} modes to occur, the Bragg grating must be tilted, or blazed, with

respect to the fiber axis. Indeed this effect has been experimentally observed by Hill et al. [1990] who determined that a tilted grating transferred power from the fundamental to the backward and forward LP_{11} modes. In other words; a grating that is perpendicular to the fiber axis can transfer power only between modes that have azimuthal symmetry.

II.2 Outline of the derivation of the coupled mode equations

The coupled mode equations describing the electric field amplitude of a single mode optical fiber with a Bragg grating written along its length, can be derived directly from the Maxwell's Equations [Marcuse, 1973 and 1974; Yariv, 1989 and Snyder and Love, 1983]. The literature in this area is very extensive and can be traced back as far as the early 1950's [Haus and Huang, 1991]. These coupled equations may take more than one format once appropriate transformations are made. The format followed here is the one adopted by Marcuse [1973 and 1974] who derived the coupled mode equations for a fiber with any number of modes. Throughout this work, it has also been assumed that coupling among bound and radiation modes is negligible.

The procedure outlined by Marcuse consists initially in accounting for the refractive index variation along the fiber length in the source-free Maxwell's equations. The fields are then decomposed in transversal and azimuthal components and in terms of the modes of an ideal waveguide with a coefficient that is dependent on the axial coordinate z. The resulting Maxwell's equations are then multiplied by the complex conjugate of the

fields and integrated over the infinite cross section of the fiber. The equations are simplified by using the orthogonality relations and lead to a set of coupled differential equations in terms of the amplitude of the ideal modes of a waveguide. Finally, the field amplitudes are written as a linear combination of backward and forward propagating modes. This, added to the fact that the z-component of the electric field of a weakly guiding fiber can be neglected, yields to the following coupled mode equations;

$$\frac{dc_{\mu}^{(+)}}{dz} = \sum_{\nu=0}^{N-1} \left(c_{\nu}^{(-)} e^{i(\beta_{\mu}+\beta_{\nu})z} + c_{\nu}^{(+)} e^{i(\beta_{\mu}-\beta_{\nu})z} \right) k_{\mu\nu} \qquad (1)$$

$$\frac{dc_{\mu}^{(+)}}{dz} = \sum_{\nu=0}^{N-1} \left(c_{\nu}^{(-)} e^{i(\beta_{\mu}+\beta_{\nu})z} + c_{\nu}^{(+)} e^{i(\beta_{\mu}-\beta_{\nu})z} \right) k_{\mu\nu} \quad . \qquad (2)$$

In the above equations, $c_{\mu}^{(+)}$ and $c_{\mu}^{(-)}$ are the amplitudes of the forward and backward propagating modes of order and rank μ, i is the imaginary constant, β the propagation constant, N the number of modes that propagate in the fiber, z the coordinate along the fiber axis and $k_{\mu\nu}$ the coupling coefficient between the modes μ and ν given by

$$k_{\mu\nu} = \frac{\omega \varepsilon_0 i}{4P} \int_0^{2\pi} \int_0^{\infty} (n_0^2 - n^2) E_{t,\nu} E_{t,\mu}^{*} r \, dr \, d\phi \quad . \qquad (3)$$

Here, ω is the circular frequency of the light, ε_0 the permitivity constant, n_0 and n the refractive index of the unperturbed and perturbed fiber, respectively, $E_{t,\nu}$ the transverse component of the electric field of the mode ν,

r and ϕ the radial and azimuthal coordinates of the fiber and P a normalization constant. Also in Eq. (3), the asterisk (*) denotes complex conjugation.

As mentioned before, Eqs. (1) through (3) are slightly different from the one presented by Marcuse for the following reason; in a weakly guiding fiber the z component of the fields can be neglected and this simplification has been used in the final result shown above.

For a single mode fiber, $N=1$ and coupling occurs only between the forward and backward propagating fields that are associated with the fundamental mode. Applying Equations (1) and (2) to a single mode fiber, the following equations are obtained

$$\frac{dc_0^{(+)}}{dz} = \left(c_0^{(+)} + c_0^{(-)} e^{2\beta_0 iz}\right) k_{00} \tag{4}$$

and

$$\frac{dc_0^{(-)}}{dz} = -\left(c_0^{(-)} + c_0^{(+)} e^{-2\beta_0 iz}\right) k_{00} \tag{5}$$

The Boundary Conditions associated with these equations can be obtained considering Figs. 1 through 4. For instance, in a semi-infinite uniform fiber a light source can excite only forward propagating modes (Figure 2). In this case, the amplitude of the backward propagating mode is zero throughout the whole fiber length. However, in a finite uniform fiber, the fiber end-face may

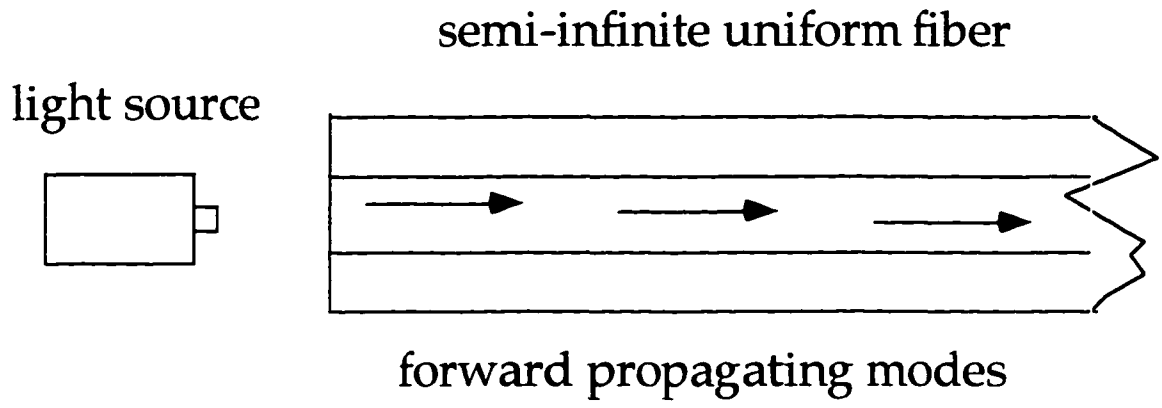

Figure 2. A semi-infinite uniform fiber excites only forward propagating modes

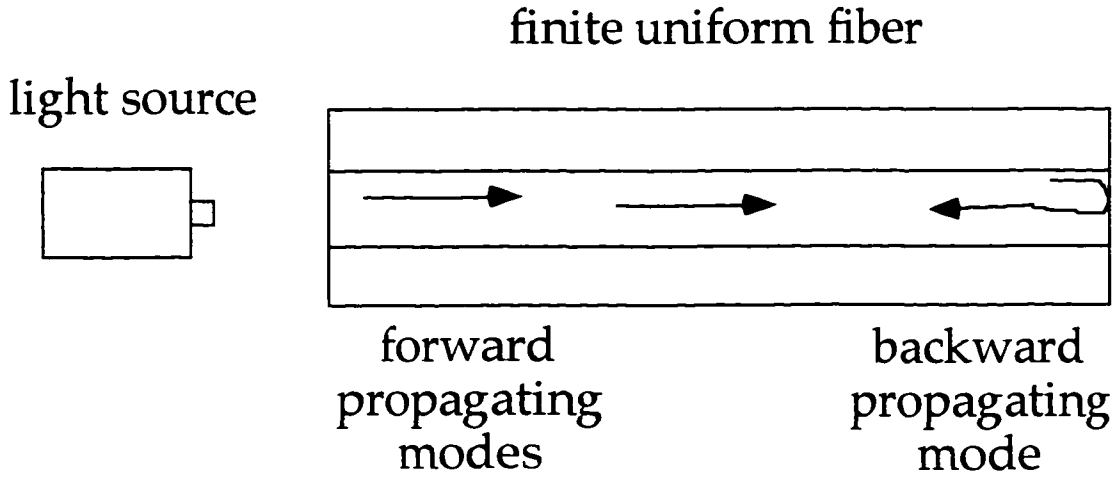

Figure 3. The end-face of a finite uniform fiber can introduce backward propagating modes through Fresnel reflections

introduce backward propagating modes through Fresnel reflections (Figure 3). In general, these reflections account to less than 4% of the total power in the modes and can be neglected. Anyhow, this kind of non-uniformity in the fiber, the glass/air interface, represents a means of transferring power from the forward to the backward propagating modes. Another way of exciting backward propagating modes would be to add a second light source at the far side of the fiber (Figure 4). A third means of doing so would be to introduce non-uniformities along the fiber length. A Bragg grating is such a kind of non-uniformity that is restricted to a finite region of the fiber (see Fig. 1) for this reason, it can introduce backward propagating modes only within the region between the source and the far side of the grating. Outside this region, i.e., at $Z \geq 1$, and assuming that Fresnel reflections at the fiber end-face can be neglected, there are no backward propagating modes. Taking that into account, the Boundary Conditions can be easily derived as

$$c_0^{(+)}(Z=0) = 1$$

and

$$c_0^{(-)}(Z=1) = 0 \quad .$$

These conditions state that the amplitude of the forward propagating mode at the input end of the fiber has been normalized to one whereas the amplitude of the associated backwards propagating mode is zero in the after-region of the grating. The above boundary conditions are very general and applies to most kind of situations.

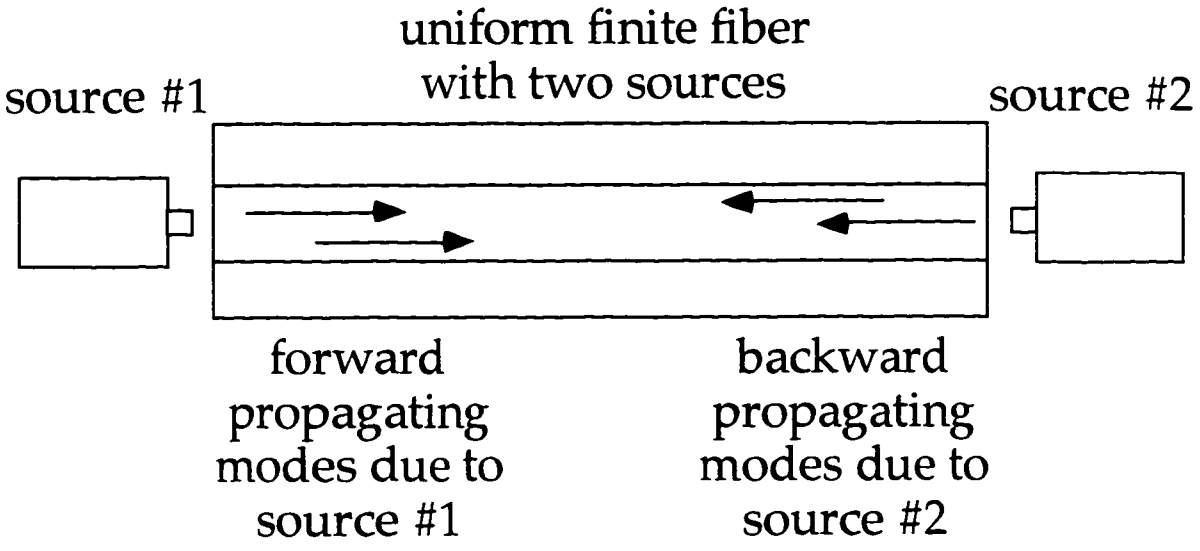

Figure 4. A second light source at the other endface of the fiber can introduce backward propagating modes in the fiber

CHAPTER III

OPTICAL FIBER BRAGG GRATINGS

III.1 Introduction

Optical fibers with a photo-induced Bragg grating was first reported by Hill et al. [1978]. At that time it was observed that light from a 488 n*m* argon laser was capable of producing a change in the refractive index of a glass fiber doped with germanium; a phenomenon called photosensitivity. Hill et al.'s experiment consisted basically in injecting the laser light into the fiber, while its output intensity would be monitored at the other end (see Fig. 5). It was observed that the output intensity would decrease with time whereas, at the input end, there was a simultaneous increase in the intensity. It was also found that the reflectivity spectrum was very narrow with a peak reflectivity at 488 n*m*. This phenomenon was thought to be due to the formation of reflection centers by the laser light. These reflection centers are basically an increase in the refractive index of the glass, the so-called phenomenon of photosensitivity. In order words, the laser light induced an index change in the fiber core along its length giving rise to a periodic variation. This variation was found to be related to the frequency of a standing wave formed inside the fiber; the standing wave formed by Fresnel reflections at the fiber end-faces. In summary, the fiber would get a permanent imprint in its refractive index due to the presence of a standing wave within the fiber. This procedure has since been known as internal writing.

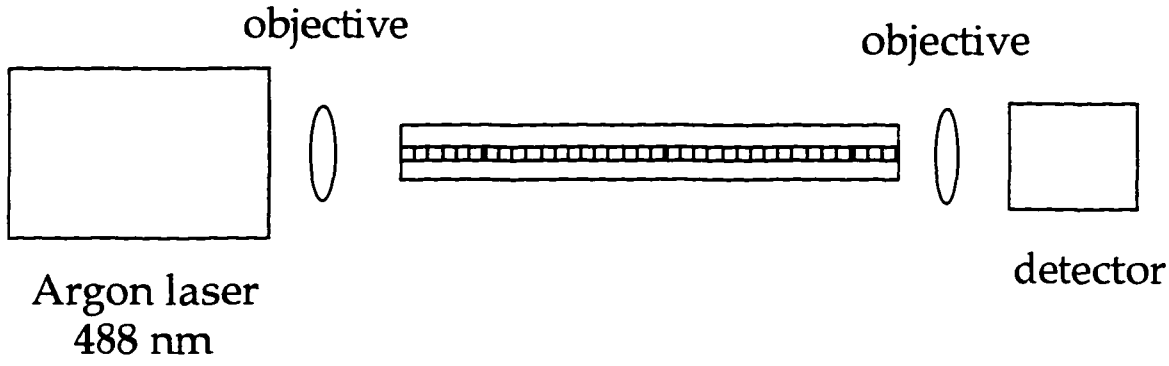

Figure 5. Experimental set-up used by Hill et al. [1978] to write a Bragg grating

III.2 Advances in Fabrication Techniques

In addition to the internal writing technique another advancement was made with the development of the external writing technique. It consists of forming Bragg gratings by transversely exposing the fiber core to two overlapping coherent, interfering UV beams [Meltz et al., 1989] of roughly 244 n*m* of wavelength (see Fig. 6). This technique has several advantages over the previous including greater efficiency, flexibility in the choice of location, period and length of the grating, and the formation of gratings of different angles with respect to the fiber axis. Indeed, it has been demonstrated that tilted gratings are capable of coupling light among bound modes that are not circularly symmetric [Hill et al., 1990], i.e., modes of different order. Among these modes, coupling does not occur whenever the grating is perpendicular to the fiber axis.

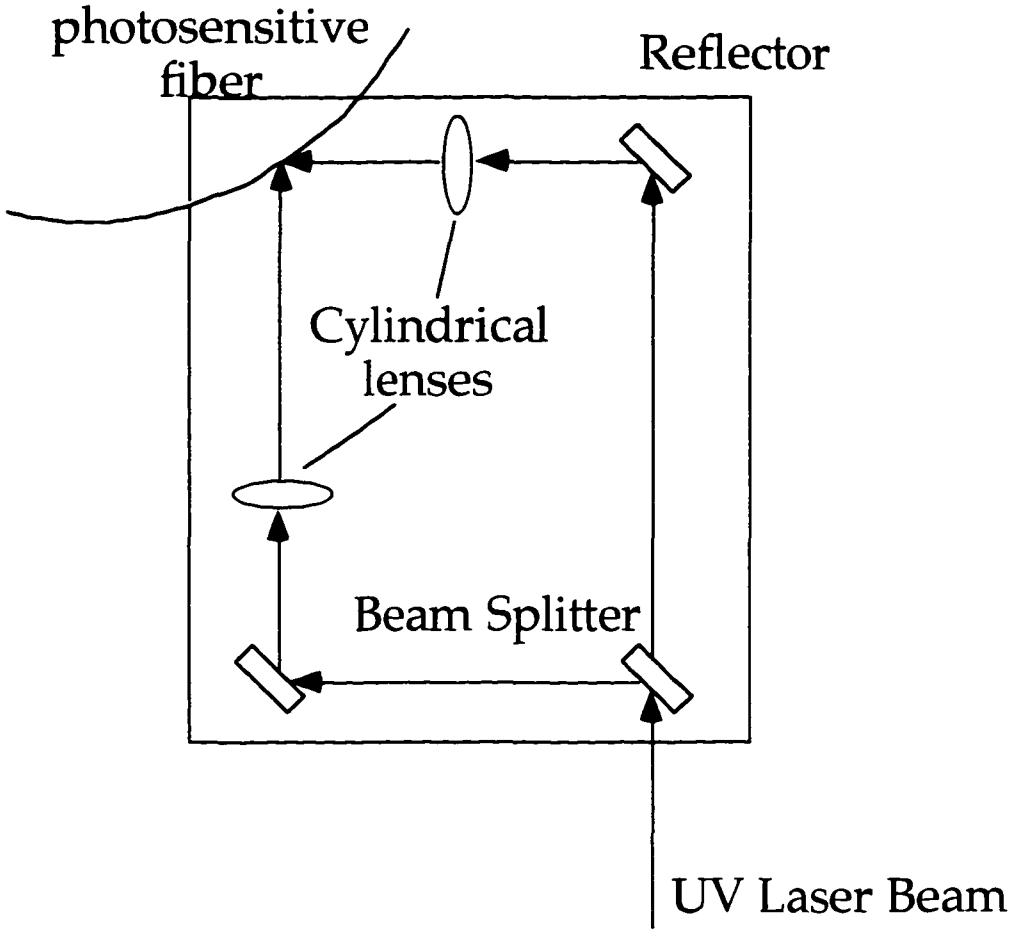

Figure 6. Experimental set-up for external writing [Meltz et al., 1989]

A third technique has also been achieved recently [Hill et al., 1993]. In this case a diffractive optical phase mask has been used to generate a near-field fringe pattern from a UV beam passing through the mask. The period of the fringes are one half that of the mask. This procedure greatly simplifies the fiber grating fabrication system avoiding fine mechanical displacements required when using the coherent UV beam technique.

Recently, Bragg gratings have been written in fibers using a a single 20 nsec excimer pulse laser [Askins et al., 1992]. This laser has a higher power output allowing a single pulse to write a grating almost instantaneously. This technique has since being used to manufacture gratings during automated fiber drawing [Askins et al., 1992 and Dong et al., 1993]

Other milestones in the fabrication of Bragg gratings include photo-sensitivity enhancement of the material by loading it with hydrogen at high pressures and the generation of gratings in fibers with dopants other than germanium such as cerium [Morey et al., 1994].

III.3 Characteristics

The periodic refractive index perturbation within the fiber acts as a mode converter; in general, the conversion is made between forward and backward propagating modes. Alternately the grating can also be designed to allow it to transfer power from the original forward propagating mode into another

forward propagating mode [Bilodeau et al., 1991]. The mode into which the power is converted depends on the grating period and the wavelength of the light used. For instance, in a single mode fiber, conversion occurs whenever the so called phase-matching condition is satisfied or

$$2\beta_{01} - \Omega = 0.$$

Similarly, in a four mode fiber, conversion between the forward fundamental mode and the backward LP_{02} mode is accomplished whenever

$$\beta_{01} + \beta_{02} - \Omega = 0$$

where β stands for the propagation constant and Ω the grating frequency. For the case of conversion into another forward propagating mode, the relation is slightly different or

$$\beta_{01} - \beta_{02} - \Omega = 0.$$

The conversion is very selective once the grating is tuned to the proper modes and the spectral distribution of the conversion is narrow as well. Typical values of the bandwidth of the reflection and transmission peaks are of the order of 1 nm .

Table 1. Optical fiber dopants for optical fiber lasers.

dopant	paper(s)
Erbium	Mears et al., 1987; Zyskind, et al., 1992; Ball and Morey, 1992; Sejka et al., 1995
Neodymium	Reekie et al., 1986; Mear et al., 1985; Ainsle et al., 1988
Thulium	Esterowitz et al., 1988; Allen and Esterowitz, 1989
Holmium	Brierley et al., 1988; Hanna et al., 1989
Ytterbium	Asseh et al., 1995; Hanna et al., 1988
Samarium	Farries et al., 1989
Praseodymium	Percival et al., 1989 and Ohishi et al., 1992

III.4 Devices

Several optical fiber Bragg devices have been envisioned such as optical fiber lasers, fixed and tunable filters, mode converters and strain and temperature sensors [3M, 1996; Morey et al., 1994 and Morey et al., 1989]. In what follows each of these devices is briefly discussed.

III.4.1 Optical fiber lasers

Lasing conditions in an optical fiber Bragg grating can be achieved by using the grating as a feedback mechanism, a fiber dopant for the gain medium and a pump source for excitation. There are several optically active dopants for fiber lasers reported in the literature (see Table 1); some of them are appropriate for silica whereas others can be used with fluoride fibers. The pumping mechanism can be made with another laser, such as Ti:sapphire, at an excitation wavelength of 980 *nm* [Ball and Morey, 1992] whereas tunability can be achieved by applying axial strain to the fiber in its grating region [Ball and Morey, 1992]. The axial strain basically changes the grating period and the fiber refractive index by a small amount producing a shift in the Bragg wavelength. This shift can be as high as 10 *nm* (see Chapter VII). An optical fiber Bragg grating laser basically can be modelled as a resonant cavity with gain [Yariv, 1989]. The coupled mode equations generated are very similar in format to the coupled mode equations of a fiber without gain.

III.4.2 Optical fiber filters and mode converters

A Bragg grating within the fiber acts as a wavelength-selective reflector. A wavelength selective reflector is virtually a mode converter that converts the power in the forward propagating modes into the backward propagating modes. This application was first reported by Hill et al., [1978]. The peak wavelength of the reflection filter is determined by the period of the grating in accordance with the Bragg condition (see Eq. (96)), i.e., on the order of $10^{-6}m$. Figure 7 is a plot of the reflectivity spectrum of a single-mode, single grating fiber, against the wavelength; the plot is given by Eq. (27). This result compares very well with experiments [Limberger et al., 1993]. As it can be seen the filter is very wavelength selective with a bandwidth on the order of 2 nm.

This kind of fiber can also be used as a mode converter among forward propagating modes [Hill et al., 1990; Bilodeau et al., 1991] with the difference that the grating period is on the order of $10^{-4}m$, i.e., three orders of magnitude longer than the period of a reflector. A typical experimental set-up for a mode converter is shown in Fig. 8; it is composed of a light source, a few mode fiber, a mode stripper and an optical spectrum analyser, OSA. Light from a broadband source is introduced into the fiber where a mode stripper strips the higher order modes allowing only the fundamental mode to propagate through it. Once the light reaches the grating, some of the power is transferred from the fundamental mode to a higher order mode, such as the LP_{02}. Another mode stripper is introduced in the far end of the grating stripping the fiber from the higher order modes. A spectrum analyser

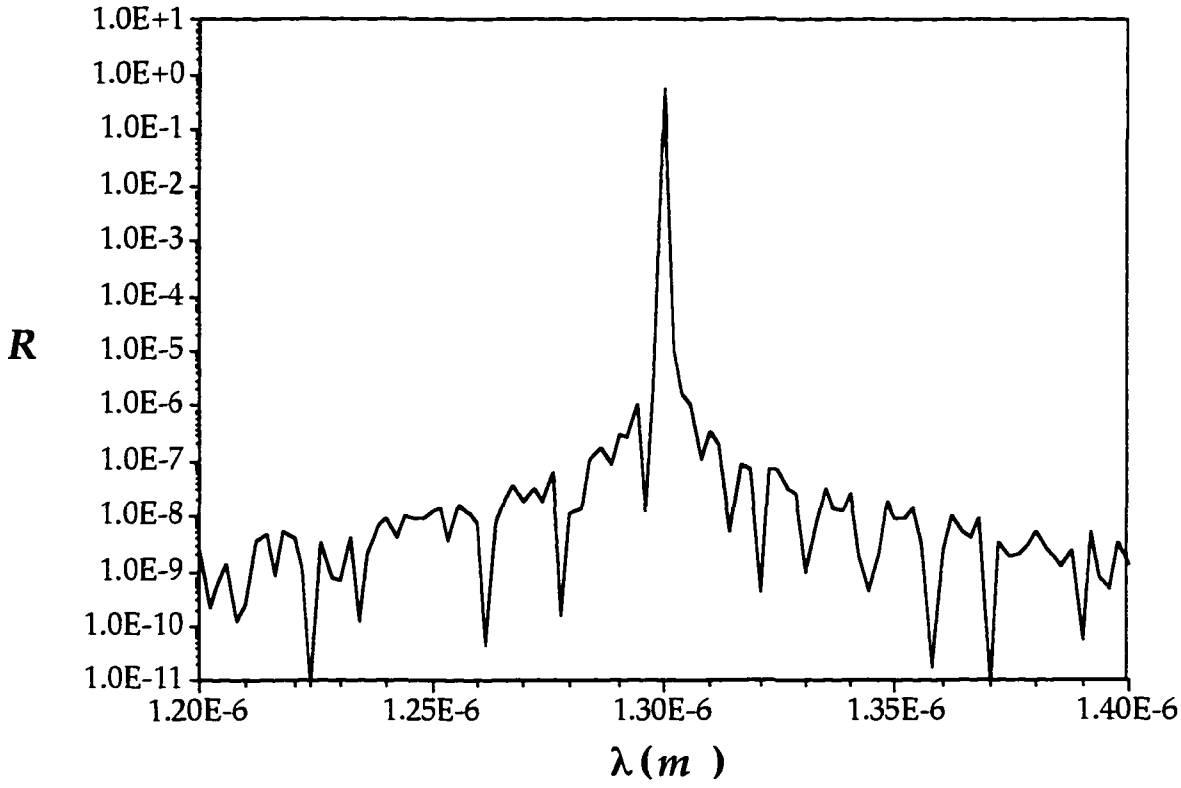

Figure 7. Reflection spectrum of a single Bragg grating at wavelength 1.3 μm. The normalized coupling constant was assumed to be 2.0, n_{core}=1.46 and L=0.03 m

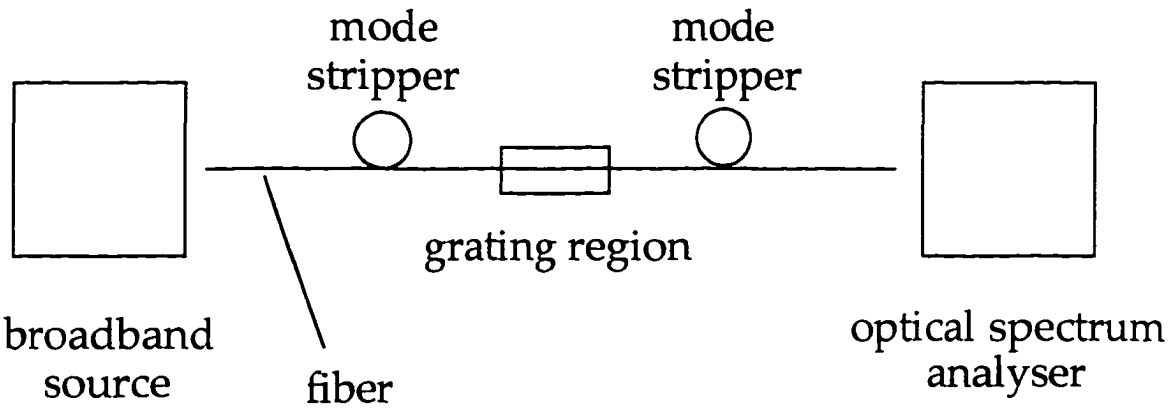

Figure 8. Experimental set-up for a mode converter

determines the final output as a function of the wavelength. Since the coupling between the fundamental and higher order modes occurs mostly within certain values of the wavelength, the output read by the OSA will have some gaps in it. Typical outputs are shown in Hill et al. [1990] and Bilodeau et al. [1991].

III.4.3 Optical fiber sensors

Another application of Bragg grating fibers is in the area of optical sensing; such as strain and temperature distributed sensing. Mechanical and thermal strain, provokes a shift in the Bragg wavelength [Xu et al., 1994; Kersey and Morey, 1993 and Chapter VII] in the same way that they shift the phase in a

Mach-Zender sensor. This shift is at most 10n*m* for coupling between forward and backward propagating modes and can be up to three orders of magnitude longer for coupling among forward propagating modes. By monitoring this shift, strain and temperature variation can be determined. This effect is due basically to changes in the fiber length and refractive index. Chapter VII has a detailed derivation of how much shift occurs once mechanical and thermal strain is applied to a Bragg grating optical fiber.

Actual distributed strain can be accomplished by writing several gratings along the length of the fiber, with different grating periods. In this case the shift would be around the Bragg wavelength of each grating –the locations of which are known before hand. Another technique consists in writing several similar gratings along the length of the fiber and measure the shift of each one by using a Fourier transform. These techniques are capable of determining different strain locations along the length of the fiber.

III.5 Summary

Since its discovery in 1978 optical fiber Bragg gratings have found applications in several fields. In this Chapter a brief outline of the devices envisioned was given so the reader can appreciate the usefulness of this new technology. There are several other applications that have not been mentioned such as wavelength division multiplexing, optical fiber chemical sensors etc.

CHAPTER IV

COUPLED EQUATIONS OF AN OPTICAL FIBER WITH A SINGLE BRAGG GRATING

IV.1 Introduction

For the case of a fiber with a single Bragg grating, the refractive index n is given by

$$n = n_0 + \delta n \left(1 + \cos\left(z\,\Omega\right)\right) \quad .$$

where δn is the index modulation and Ω is the frequency of variation of the refractive index. The above relation for the refractive index yields a very complicated solution of the coupled mode equations. However, it has been found that the *approximate* relation

$$n = n_0 + \delta n \cos(z\,\Omega) \tag{6}$$

yields much simpler solutions. Furthermore, δn is a very small quantity, i.e., $\delta n < 10^{-2}$ which implies that Eq. (6) is a very good approximation to the refractive index in a Bragg grating fiber. In addition to that, Eq. (6) has been used over and over again in the solutions of the Bragg grating fiber resulting in very good agreement with experimental results [Lam and Garside, 1981 and Limberger et al., 1993]. Because of these three reasons, it has been chosen to use Eq. (6) as the relation for the refractive index solution.

Substituting Eq. (6) into (3) and taking into account that δn is very small, on the order of 10^{-4} to 10^{-2}, the squared terms can be neglected. The coupling constant can then be rewritten as

$$k_{00} = \overline{k_{00}} \cos(z\,\Omega) \tag{7}$$

where

$$\overline{k_{00}} = -\frac{\delta n\, \omega\, \varepsilon_0\, n_0\, i}{2P} \int_0^{2\pi} \int_0^{\infty} |E_{t,0}|^2\, r\, dr\, d\phi \quad . \tag{8}$$

Introducing Eq. (7) into Eqs. (4) and (5), and expanding the circular function in terms of complex exponentials, the coupled mode equations reduce to

$$\frac{dc_0^{(+)}}{dz} = \frac{\overline{k_{00}}}{2}\left[\left(e^{i(2\beta_0+\Omega)z} + e^{i(2\beta_0-\Omega)z}\right) c_0^{(-)} + \left(e^{-i\Omega z} + e^{i\Omega z}\right) c_0^{(+)}\right] \tag{9}$$

$$\frac{dc_0^{(-)}}{dz} = -\frac{\overline{k_{00}}}{2}\left[\left(e^{-i\Omega z} + e^{i\Omega z}\right) c_0^{(-)} + \left(e^{-i(2\beta_0+\Omega)z} + e^{-i(2\beta_0-\Omega)z}\right) c_0^{(+)}\right] \tag{10}$$

Introducing L as the length of the Bragg grating and defining the real normalized parameters

$$Z = \frac{z}{L} \quad , \tag{11}$$

$$\alpha = (2\beta_0 + \Omega) L , \tag{12}$$

$$\gamma = (2\beta_0 - \Omega) L \quad \text{and} \tag{13}$$

$$C_{00} = L \overline{k_{00}} i \quad , \tag{14}$$

Eqs. (9) and (10) reduce to the following

$$\frac{dc_0^{(+)}}{dZ} = -\frac{C_{00}}{2} i \left[\left(e^{\alpha i Z} + e^{\gamma i Z} \right) c_0^{(-)} + \left(e^{-(\alpha-\gamma) i Z/2} + e^{(\alpha-\gamma) i Z/2} \right) c_0^{(+)} \right] \tag{15}$$

$$\frac{dc_0^{(-)}}{dZ} = \frac{C_{00}\, i}{2} \left[\left(e^{-(\alpha-\gamma) i Z/2} + e^{(\alpha-\gamma) i Z/2} \right) c_0^{(-)} + \left(e^{-\alpha i Z} + e^{-\gamma i Z} \right) c_0^{(+)} \right] \tag{16}$$

In the above, γ is the normalized phase matching parameter and C_{00} the normalized coupling constant. The normalized phase matching parameter determines the wavelength at which coupling is maximum among modes whereas the the normalized coupling constant determines how strong is coupling among modes.

IV.2 The Asymptotic Solution

A simple asymptotic solution of Eqs. (15) and (16) can be obtained for large values of α. This solution applies to the case in which $\alpha >> 1$ and $\alpha >> \gamma$ or, more specifically, $\alpha > 100$ and $\alpha/\gamma > 100$. For bound modes of an optical fiber, the

first condition always hold because of the order of magnitude of the wavelength and the grating period. More specifically, large values of α are associated with optical devices which have wavenumbers on the order of $10^6 m^{-1}$. This can be appreciated by analysing Eq. (12) which indicates that α is on the order of 10^5 for grating lengths of a few centimeters, refractive index values around 1.5 and wavelengths in the visible region of the spectrum.

In general, the relation $\alpha/\gamma>100$ is satisfied specially in the neighborhood of the phase matching condition where $\gamma\approx 0$. Similarly, from its very definition, γ will always be smaller than α. Taking these facts into consideration, the asymptotic solution can now be derived. By integrating both sides of Eqs. (15) and (16), it is clear that the integrals involved are of the form

$$I = \int e^{a i Z} c_0^{(\pm)} \, dZ \tag{17}$$

where a can be either $\pm\alpha$, $\pm\gamma$ or $\pm(\alpha-\gamma)/2$. Integration by parts of Eq. (17), generates an expression with coefficient $1/a$ or

$$\int e^{a i Z} c_0^{(\pm)} \, dZ = -\frac{i c_0^{(\pm)} e^{a i Z}}{a} + \frac{i}{a} \int e^{a i Z} \frac{dc_0^{(\pm)}}{dZ} \, dZ \tag{18}$$

Further integration by parts of the remaining integral generates additional powers of $1/a$ with an integrand directly proportional to the derivative of the amplitude of the electric field. This quantity will always be finite no matter the values of its parameters and, for this reason, the second term in the right hand side of Eq. (18) will become negligible whenever $\alpha \Rightarrow \infty$ or

$$\lim_{\alpha \to \infty} \int e^{\pm(\alpha-\gamma)iZ/2} c_0^{(\pm)} dZ = \lim_{\alpha \to \infty} \int e^{\pm \alpha i Z} c_0^{(\pm)} dZ \cong 0 \quad . \quad (19)$$

This approximation, the so-called Asymptotic Approximation, neglects the higher frequency terms in the solution of the coupled mode equations [Snyder and Love, 1983]. So, applying Eq. (19) to the integrals of Eqs. (15) and (16), reverting this result to a set of differential equations and adding a zero subscript to the fields to distinguish them from the exact solution, the coupled differential equations reduce to

$$\frac{dc_{0,0}^{(+)}}{dZ} = -\frac{C_{00}\, i}{2} e^{\gamma i Z} c_{0,0}^{(-)} \quad (20)$$

and

$$\frac{dc_{0,0}^{(-)}}{dZ} = \frac{C_{00}\, i}{2} e^{-\gamma i Z} c_{0,0}^{(+)} \quad . \quad (21)$$

The solution of this set of equations is obtained by turning them into a single second order differential equation in terms of either $c_{0,0}^{(+)}$ or $c_{0,0}^{(-)}$ such as

$$\frac{d^2 c_{0,0}^{(+)}}{dz^2} - i\gamma \frac{dc_{0,0}^{(+)}}{dz} - \frac{C_{00}^2}{4} c_{0,0}^{(+)} = 0 \quad .$$

The solution of the above equation is straight-forward and can be obtained in terms of exponential functions. Next the Boundary Condition for $c_{0,0}^{(+)}$ is applied and the resulting equation is substituted into Eq. (20). Finally the Boundary Condition for $c_{0,0}^{(-)}$ is also applied leading to the final solution

$$c_{0,0}^{(+)} = \frac{\left\{\eta\, i \cos\left[\frac{\eta\,(1-Z)}{2}\right] - \gamma \sin\left[\frac{\eta\,(1-Z)}{2}\right]\right\} e^{i\gamma Z/2}}{\eta\, i \cos\left(\frac{\eta}{2}\right) - \gamma \sin\left(\frac{\eta}{2}\right)} \tag{22}$$

and

$$c_{0,0}^{(-)} = \frac{C_{00} \sin\left[\frac{\eta\,(1-Z)}{2}\right] e^{-i\gamma Z/2}}{\eta\, i \cos\left(\frac{\eta}{2}\right) - \gamma \sin\left(\frac{\eta}{2}\right)} \tag{23}$$

where

$$\eta = \sqrt{\gamma^2 - C_{00}^2}\ . \tag{24}$$

This result can be directly verified by substituting them into Eqs. (20) and (21). It is important to point out that the Boundary Conditions of the asymptotic approximation are the same for the exact field solution.

IV.3 Comparison between asymptotic and numerical solutions

In order to determine the validity of the asymptotic approximation a comparison was made with the numerical solution. The procedure used consisted basically of four steps;

1. the original coupled mode equations, Eqs. (15) and (16), were broken down into four separate equations describing the real and imaginary portions of the fields;

2. then the *asymptotic approximation* was used to determine the initial value of the backward propagating field at Z=0 (the initial value of forward propagating field is already given by the initial condition);

3. with the values calculated in 2, the problem was then treated as an initial value problem using the Runge-Kutta method [Maron, 1982, Chapter 8, subroutine RKF4 and Prescience, 1994]. The final result was a numerical solution of the amplitude fields throughout the Z interval, i.e., 0<Z<1, and finally

4. the power in the backward propagating mode given by

$$P = |c_0^{(-)}|^2 \tag{25}$$

was obtained for both numerical and asymptotic solutions and compared between each other.

This method can be thought of as a slight variant of the shooting method in which an arbitrary value of the backward propagating field is chosen at Z=0. Using this value the differential equation is then solved as an initial value problem throughout the domain of values of Z. The final numerical solution at Z=1 is then compared with the actual Boundary Conditions and, depending on the outcome of this comparison, it is chosen either to refine the original value of the backward propagating field or to end the iteration process. In the procedure adopted here, the second step or refinement in the initial value, is not undertaken because the intention here is only to determine whether the numerical and approximate results are compatible

between each other. Furthermore, additional refinement would result in extensive computer time. Some of the results are presented in what follows.

Using the procedure discussed above, several plots of the numerical and approximate solutions were made against the normalized longitudinal coordinate. Figures 9 and 10 display some of these results for a typical value of α, α =100,000 (see Appendix C), and a few additional values of γ and C_{00}. It can be seen from Fig. 9 that the numerical solution can hardly be distinguished from the asymptotic one for all three cases. The exception is the case in which γ=10,000. At this value both curves differ slightly but the coupling is very small as well. The small difference is due to the value of γ which is only 1/10 of the value of α. If γ were to become higher the difference would increase even more since the asymptotic solution was derived for $\alpha>>\gamma$. Also, notice that the higher the modulus of η, the lower the power transferred to the backward propagating mode, i.e., the higher the η the lower the coupling between modes.

In Fig. 10, the transferred power was plotted against Z for γ=0. This γ value corresponds to the so-called phase matching condition in which maximum power is transferred between the modes. From Fig. 10, it can readily be seen that the higher the value of the normalized coupling constant C_{00}, the lower the Z-value at which the numerical and asymptotic solutions start to diverge. For instance, whenever C_{00} =5, both solutions diverge at Z=0.7, whereas for C_{00}=7, they diverge at Z=0.5. It is not clear why there is this difference between the numerical and asymptotic values. One explanation would be the possibility that the numerical solution diverges for these particular parametric values. Another explanation might be that the asymptotic solution fails in this parametric region as well.

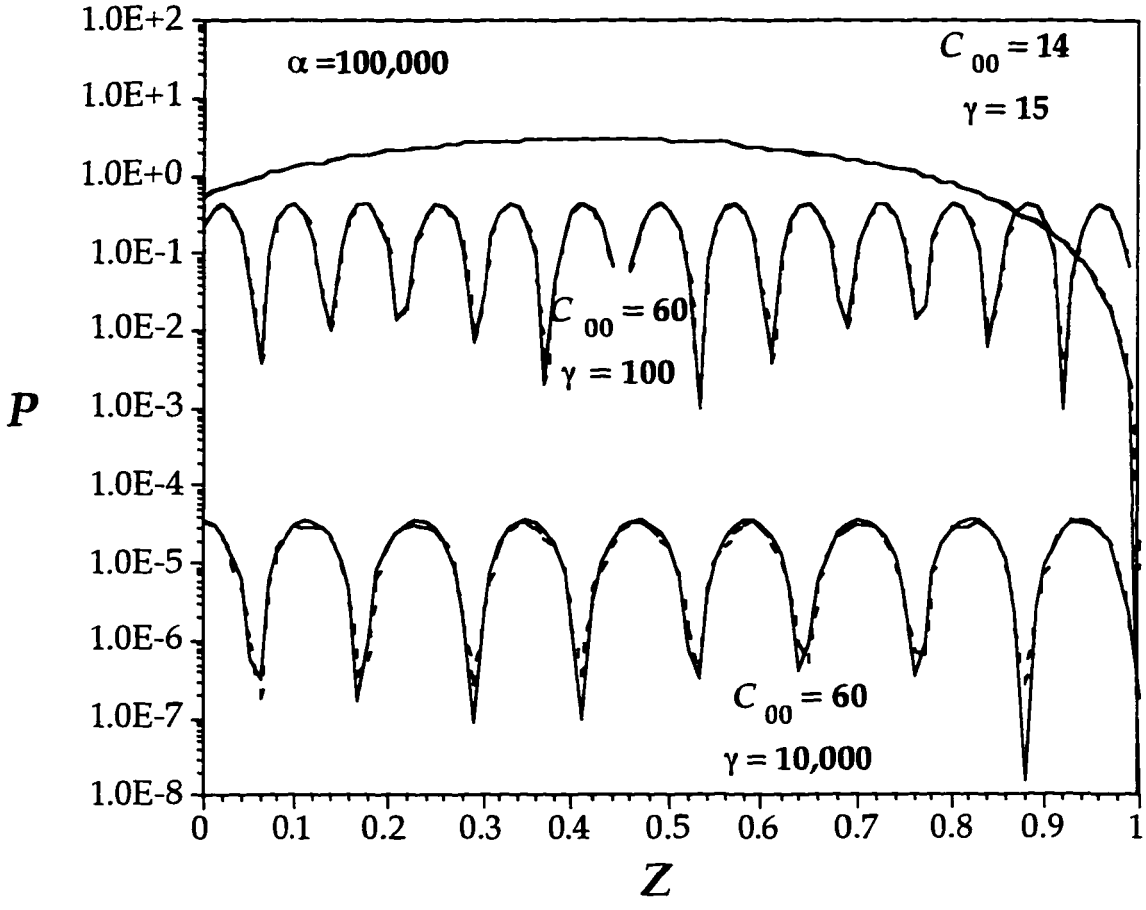

Figure 9. Numerical and asymptotic solutions for the transferred power against the normalized position.

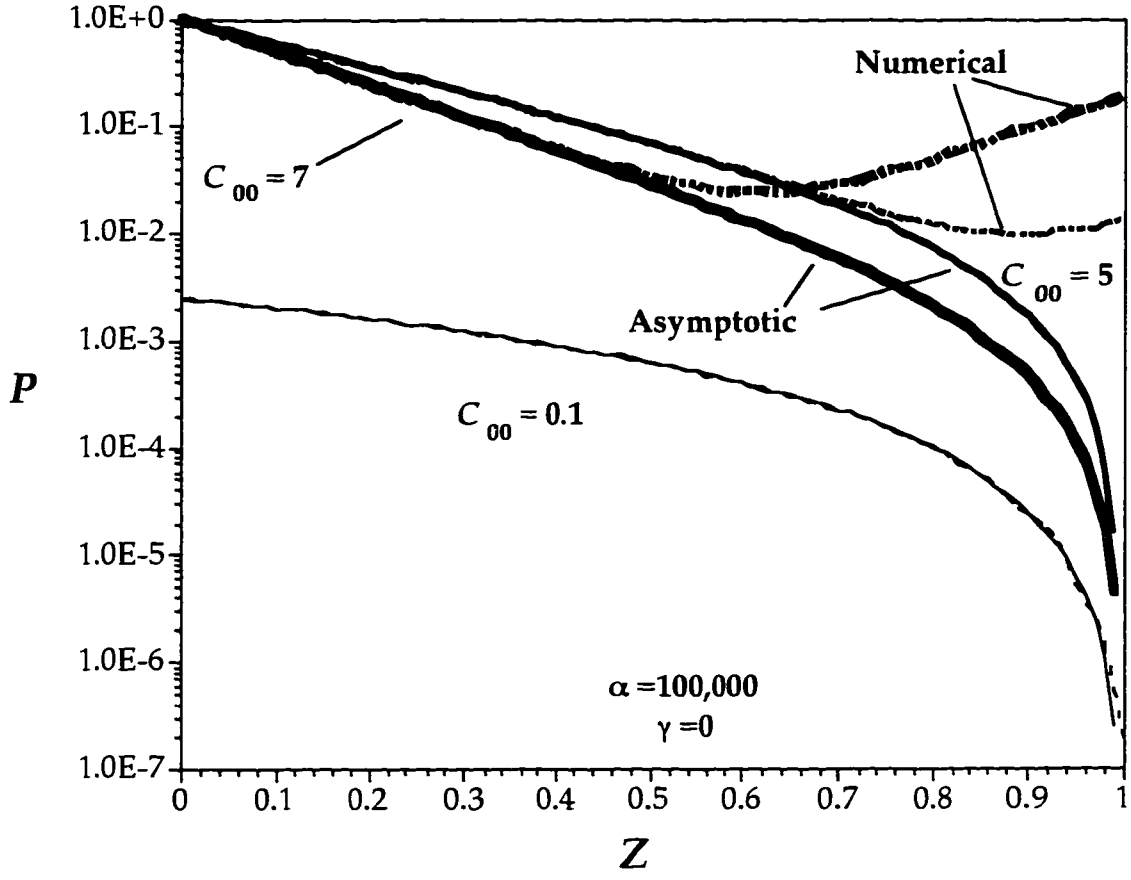

Figure 10. Numerical (dashed curves) and asymptotic (solid curves) solutions for the transferred power against the normalized position in an optical fiber Bragg grating nearby the phase matching condition, γ=0. The higher the value of the coupling constant, the more the numerical and approximate solutions deviates from each other.

IV.4 Reflectivity of a single mode fiber with a single Bragg grating

One parameter of particular interest in an optical fiber Bragg grating is the reflectivity of the grating. Once light in the forward propagating mode reaches the Bragg grating, some of its power is transferred to the backward propagating mode. This power transfer is virtually a reflection. Accordingly, the reflectivity of a Bragg grating is related to the power in the backward and forward modes [Lam and Garside, 1983] at Z=0 or

$$R = \left. \frac{|c_0^{(-)}|^2}{|c_0^{(+)}|^2} \right|_{Z=0} . \tag{26}$$

Using Eq. (26) and the result for the asymptotic solution, Eq. (26) reduces to

$$R_0 = \frac{C_{00}^2 \sin^2\left(\frac{\eta}{2}\right)}{\left| \gamma^2 - C_{00}^2 \cos^2\left(\frac{\eta}{2}\right) \right|} \tag{27}$$

where R_0 is the reflectivity obtained using the asymptotic solution. Figure 11 is a contour plot of the reflectivity against the normalized coupling constant and the normalized phase matching parameter. As it can be seen, the reflectivity increases with the normalized coupling constant and is maximum at the phase matching condition γ=0; a result well known in the literature [Lam and Garside, 1981; Haus and Huang, 1991 etc].

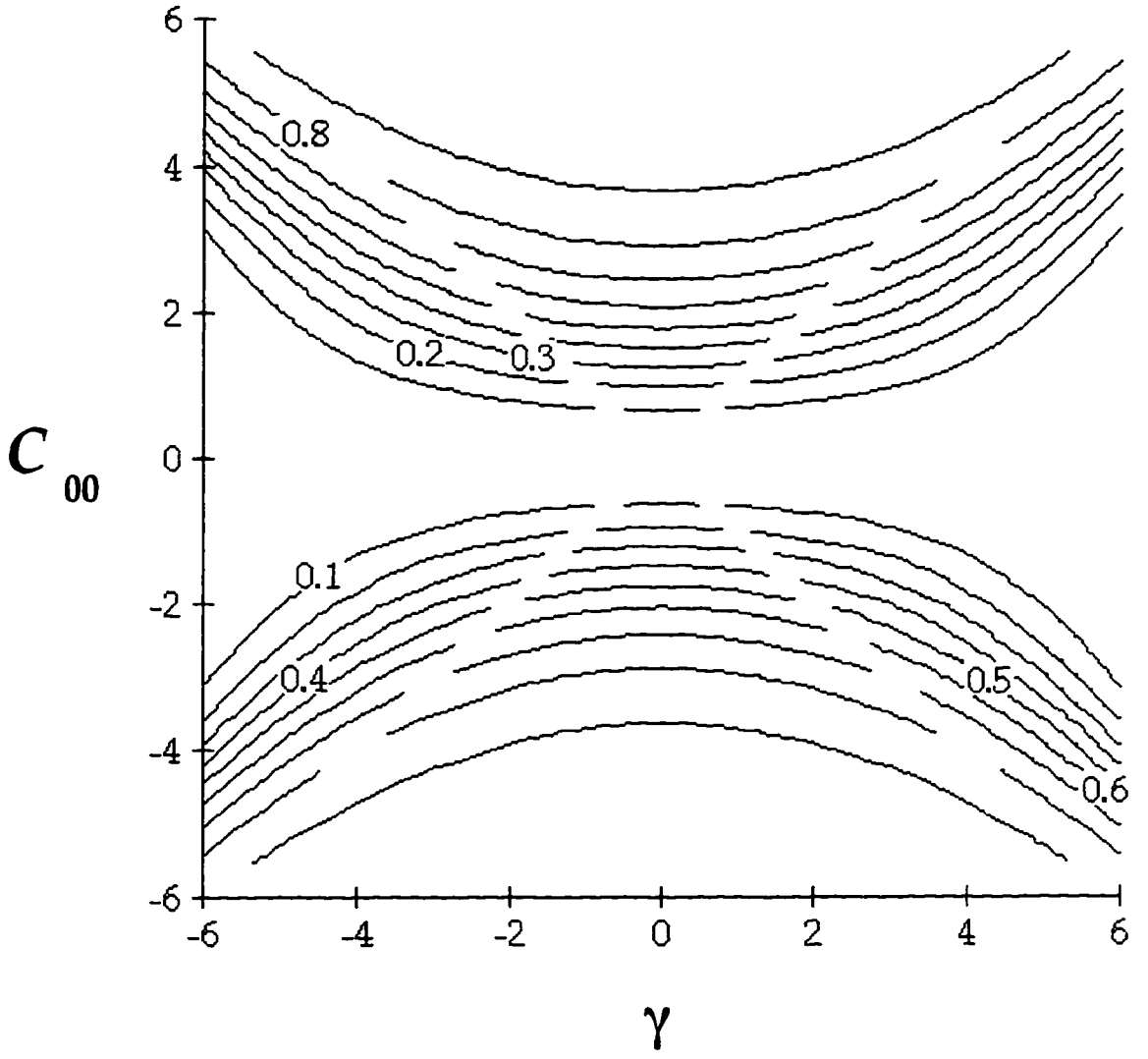

Figure 11. Contour plot of the Reflectivity against the normalized coupling constant and the normalized phase matching parameter for a single Bragg grating optical fiber. At a given value of the coupling constant, the reflectivity is maximum at $\gamma=0$.

IV.5 Summary

In this section the asymptotic solution was reformulated for a single mode fiber with a single grating. A step by step mathematical procedure was presented to arrive at a final approximate solution. The approximate solution was then compared with the numerical solution using the Runge-Kutta method. It was found that both analytical and numerical solution agree very well whenever the normalized coupling constant is less than 5. At high values of the coupling constant these two solutions diverge. The disagreement in this region is thought to be due to the possibility that the numerical solution diverges for high values of the normalized coupling constant. Using the asymptotic solution for the fields the reflectivity was then plotted as a function of its two parameters.

CHAPTER V

COUPLED EQUATIONS OF AN OPTICAL FIBER WITH DUAL BRAGG GRATINGS

V.1 Introduction

The derivation of the solutions of the coupled mode equations of an optical fiber with two Bragg gratings is similar to the previous case yet more involved. For this case, a second Bragg modulation of frequency $\Omega_2 \neq \Omega_1$ is present. Taking that into account, the refractive index n can be written as

$$n = n_0 + \delta n \left[\cos\left(z\,\Omega_1\right) + \cos\left(z\,\Omega_2\right)\right] \tag{28}$$

where it has been assumed that the amplitude modulation of the second grating is equal to the amplitude modulation of the first. Substituting this result into the coupled mode equations, they reduce to

$$\frac{dc_0^{(+)}}{dz} = \frac{\overline{k_{00}}}{2}\left[c_0^{(-)}\sum_{m=1}^{2}\left(e^{i(2\beta_0+\Omega_m)z} + e^{i(2\beta_0-\Omega_m)z}\right) + c_0^{(+)}\sum_{m=1}^{2}\left(e^{-i\Omega_m z} + e^{i\Omega_m z}\right)\right] \tag{29}$$

$$\frac{dc_0^{(-)}}{dz} = -\frac{\overline{k_{00}}}{2}\left[c_0^{(+)}\sum_{m=1}^{2}\left(e^{-i(2\beta_0+\Omega_m)z} + e^{-i(2\beta_0-\Omega_m)z}\right) + c_0^{(-)}\sum_{m=1}^{2}\left(e^{-i\Omega_m z} + e^{i\Omega_m z}\right)\right] \tag{30}$$

where $\overline{k_{00}}$ is given by Eq. (8). The above equations can now be rewritten in terms of the normalized parameters defined previously or

$$\frac{dc_0^{(+)}}{dZ} = -\frac{C_{00}\, i}{2}\left(c_0^{(-)}\sum_{m=1}^{2}\left(e^{\alpha_m iZ} + e^{\gamma_m iZ}\right) + c_0^{(+)}\sum_{m=1}^{2}\left(e^{-(\alpha_m-\gamma_m)\, iZ\,2} + e^{(\alpha_m-\gamma_m)\, iZ\,2}\right)\right) \tag{31}$$

and

$$\frac{dc_0^{(-)}}{dZ} = \frac{C_{00}\, i}{2}\left(c_0^{(+)}\sum_{m=1}^{2}\left(e^{-\alpha_m iZ} + e^{-i\gamma_m iZ}\right) + c_0^{(-)}\sum_{m=1}^{2}\left(e^{-(\alpha_m-\gamma_m)\, iZ\,2} + e^{(\alpha_m-\gamma_m)\, iZ\,2}\right)\right) \tag{32}$$

where

$$\alpha_m = (2\beta_0 + \Omega_m)\, L \tag{33}$$

and

$$\gamma_m = (2\beta_0 - \Omega_m)\, L \cdot \tag{34}$$

V.2 The Modified Asymptotic Solution

In the case of an optical fiber with two Bragg gratings, the set of differential equations has a total of five parameters in which the parametric values of α_{rr} are still large, i.e. $\alpha_{rr} >> 1$ and $\alpha_{rr} >> \gamma_{rr}$. So, if these conditions are applied to Eqs. (31) and (32), the following simplified result, similar to Eqs. (20) and (21), is obtained

$$\frac{dc_0^{(+)}}{dZ} \cong -\frac{C_{00}\, i}{2} c_0^{(-)} \sum_{m=1}^{2} e^{\gamma_m i Z} \tag{35}$$

and

$$\frac{dc_0^{(-)}}{dZ} \cong \frac{C_{00}\, i}{2} c_0^{(+)} \sum_{m=1}^{2} e^{-\gamma_m i Z} \quad . \tag{36}$$

Unlike Eqs. (20) and (21), these two coupled differential equations can not be solved exactly. However, it is still possible to obtain an exact solution if the additional assumptions $|\gamma_2| >> |\gamma_1|$ and $|\gamma_2| >> 1$ are introduced. In practice these assumptions means that the Bragg wavelength of the two gratings are at least $10nm$ apart. These assumptions lead to what has been called the modified asymptotic solution which will be used to generate the first order approximation in $1/\gamma_2$. The procedure adopted is the one outlined in the Appendix A and B. Doing so, the following solutions for the two Bragg grating fiber are obtained

$$c_{0,0}^{(+)} = \frac{\left\{\eta_1 \, i \cos\left[\frac{\eta_1 (1-Z)}{2}\right] - \gamma_1 \sin\left[\frac{\eta_1 (1-Z)}{2}\right]\right\} e^{i\gamma_1 Z/2}}{\eta_1 \, i \cos\left(\frac{\eta_1}{2}\right) - \gamma_1 \sin\left(\frac{\eta_1}{2}\right)} \tag{37}$$

and

$$c_{0,0}^{(-)} = \frac{C_{00} \sin\left[\frac{\eta_1 (1-Z)}{2}\right] e^{-i\gamma_1 Z/2}}{\eta_1 \, i \cos\left(\frac{\eta_1}{2}\right) - \gamma_1 \sin\left(\frac{\eta_1}{2}\right)} \tag{38}$$

where

$$\eta_1 = \sqrt{\gamma_1^2 - C_{00}^2} \, . \tag{39}$$

Again, it must be emphasized that this solution is valid only in the region where $|\gamma_2| \gg |\gamma_1|$ and $|\gamma_2| \gg 1$, i.e., in the region nearby the Bragg wavelength of the first grating. If the condition were to be inverted to read $|\gamma_1| \gg |\gamma_2|$ and $|\gamma_1| \gg 1$ the γ_1 term would have to be replace with γ_2 in Eqs. (37) and (38).

The first order correction $c_{0,1}^{(\pm)}$ on $1/\gamma_2$ follows from the Piccard Method (Appendix A) and is given by

$$\frac{dc_{0,1}^{(+)}}{dZ} = -\frac{C_{00}}{2} i \left(c_{0,0}^{(-)} \sum_{m=1}^{2} \left(e^{\alpha_m i Z} + e^{\gamma_m i Z} \right) + c_{0,0}^{(+)} \sum_{m=1}^{2} \left(e^{-(\alpha_m - \gamma_m) i Z/2} + e^{(\alpha_m - \gamma_m) i Z/2} \right) \right) \tag{40}$$

$$\frac{dc_{0,1}^{(-)}}{dZ} = \frac{C_{00}\, i}{2}\left(c_{0,0}^{(+)} \sum_{m=1}^{2} \left(e^{-\alpha_m i Z} + e^{-i\gamma_m i Z}\right) + c_{0,0}^{(-)} \sum_{m=1}^{2} \left(e^{-(\alpha_m - \gamma_m) i Z/2} + e^{(\alpha_m - \gamma_m) i Z/2}\right)\right) \tag{41}$$

Integrating the above equations, using Eq. (19), and neglecting the terms that are a function of α_m, leads to the following

$$c_{0,1}^{(+)} = -\frac{C_{00}\, i}{2}\left(\int c_{0,0}^{(-)}\, e^{\,i\gamma_2 Z}\, dZ + \int c_{0,0}^{(-)}\, e^{\,i\gamma_1 Z}\, dZ\right) - c_2^{(+)} \tag{42}$$

and

$$c_{0,1}^{(-)} = \frac{C_{00}\, i}{2}\left(\int c_{0,0}^{(+)}\, e^{-i\gamma_2 Z}\, dZ + \int c_{0,0}^{(+)}\, e^{-i\gamma_1 Z}\, dZ\right) - c_2^{(-)} \tag{43}$$

Equations (86) and (87) in the Appendix B can now be used to solve the second integral in the right hand side of Eqs. (42) and (43) or

$$\int c_{0,0}^{(+)}\, e^{-\gamma_1 i Z}\, dZ = -\frac{2\, i\, c_{0,0}^{(-)}}{C_{00}} \tag{44}$$

and

$$\int c_{0,0}^{(-)}\, e^{\gamma_1 i Z}\, dZ = \frac{2\, i\, c_{0,0}^{(+)}}{C_{00}} \quad . \tag{45}$$

Again, Eqs. (91) and (92) in the Appendix B can be used to solve the remaining integrals or

$$\int c_{0,0}^{(+)} e^{-i\gamma_2 Z}\, dZ = i\left[\frac{c_{0,0}^{(+)}}{\gamma_2} + \frac{C_{00}\, c_{0,0}^{(-)}\, e^{i\gamma_1 Z}}{2(\gamma_1-\gamma_2)\gamma_2}\right] e^{-i\gamma_2 Z} \sum_{m=0}^{\infty} \frac{C_{00}^{2m}/2^{2m}}{\gamma_2^m (\gamma_1-\gamma_2)^m} \tag{46}$$

$$\int c_{0,0}^{(-)} e^{i\gamma_2 Z}\, dZ = -i\left[\frac{c_{0,0}^{(-)}}{\gamma_2} + \frac{C_{00}\, c_{0,0}^{(+)}\, e^{-i\gamma_1 Z}}{2(\gamma_1-\gamma_2)\gamma_2}\right] e^{i\gamma_2 Z} \sum_{m=0}^{\infty} \frac{C_{00}^{2m}/2^{2m}}{\gamma_2^m (\gamma_1-\gamma_2)^m} \tag{47}$$

These two solutions converge whenever

$$\frac{C_{00}^2/2^2}{|\gamma_2(\gamma_1-\gamma_2)|} < 1 \,. \tag{48}$$

Substituting Eqs. (46) and (47) into (42) and (43), taking into account that the infinite sum can be rewritten as

$$\sum_{m=0}^{\infty} \frac{C_{00}^{2m}/2^{2m}}{\gamma_2^m (\gamma_1-\gamma_2)^m} = \sum_{m=0}^{\infty} \left[\frac{C_{00}^2/4}{(\gamma_1-\gamma_2)\gamma_2}\right]^m = \left[1 - \frac{C_{00}^2/4}{(\gamma_1-\gamma_2)\gamma_2}\right]^{-1}$$

and expanding the resulting equation in powers of $1/\gamma_2$, Eqs. (42) and (43) reduce to

$$c_{0,1}^{(+)} = c_{0,0}^{(+)} + \frac{C_{00}}{2\gamma_2}\left[\frac{C_{00}\sin\left(\frac{\eta_1}{2}\right)}{\eta_1 i\cos\left(\frac{\eta_1}{2}\right)-\gamma_1\sin\left(\frac{\eta_1}{2}\right)} - c_{0,0}^{(-)} e^{\gamma_2 iZ}\right] \qquad (49)$$

and

$$c_{0,1}^{(-)} = c_{0,0}^{(-)} + \frac{C_{00}}{2\gamma_2}\left[\frac{\eta_1 e^{i(\gamma_1-2\gamma_2)/2\, i}}{\eta_1 i\cos\left(\frac{\eta_1}{2}\right)-\gamma_1\sin\left(\frac{\eta_1}{2}\right)} - c_{0,0}^{(+)} e^{-\gamma_2 iZ}\right] \quad . \qquad (50)$$

These solutions will now be used to determine the characteristics of a two Bragg grating fiber.

V.3 Comparison between approximate and numerical solutions

In order to determine the validity of Eqs. (49) and (50), they were compared with the numerical solution using the same procedure adopted in the Chapter IV. Figures 12 through 14 are typical results of a double Bragg grating nearby the phase matching condition of the first grating. In all figures, the broken lines correspond to numerical solutions whereas the continuous lines correspond to the approximate solution. As it can be seen from Figs. 12 through 14, the behaviour of the numerical solution with respect to the approximate solution is similar to the one in Fig. 10, i.e., there is a steady departure from the approximate solution at a given Z-value. The higher the normalized coupling coefficient the lower the Z-value at which the numerical solution departs from the approximated solution. Also, in Fig. 12, there is a modulation in the amplitude of the curve throughout the values of

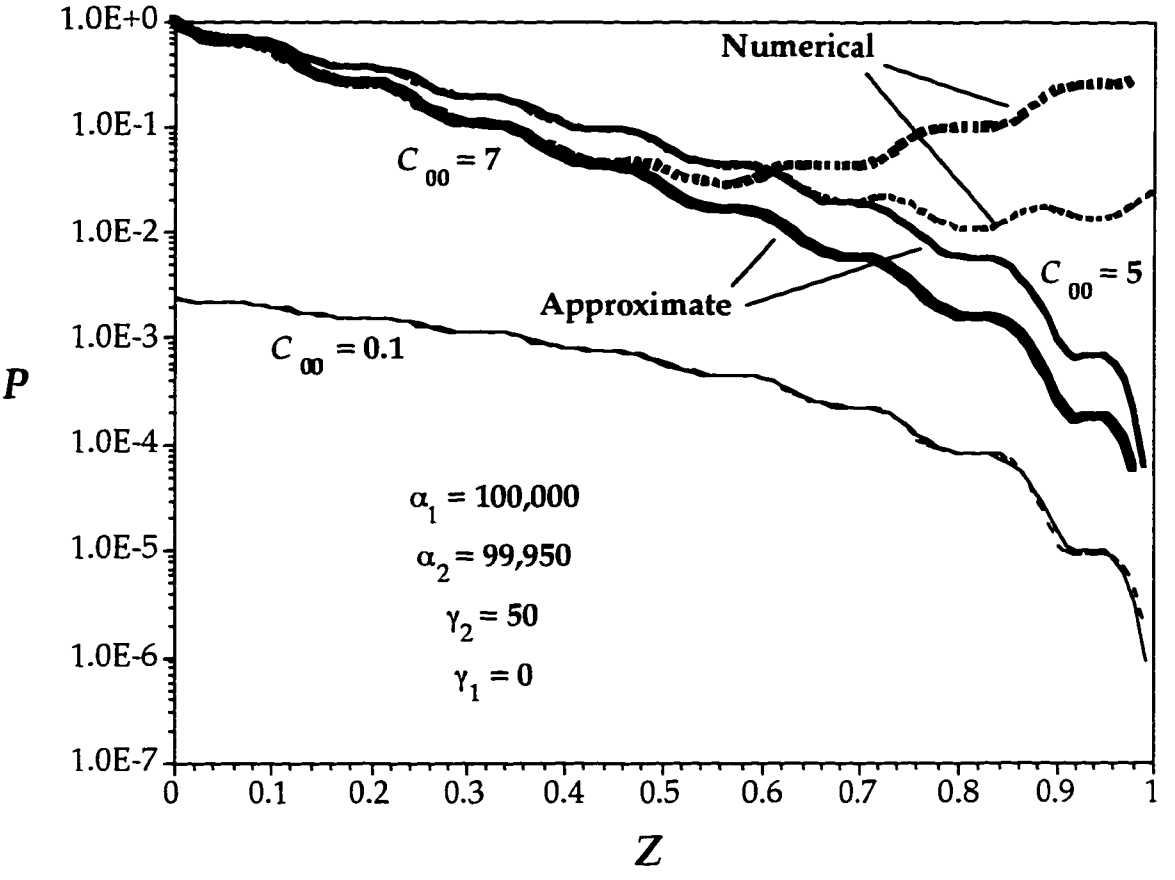

Figure 12. Comparison between numerical (dashed lines) and approximate (solid lines) solutions for an optical fiber with two co-located Bragg gratings (α_1=100,000, α_2=99,950, γ_1=0, γ_2=50 and C_{00}=0.1, C_{00}=5 and C_{00}=7).

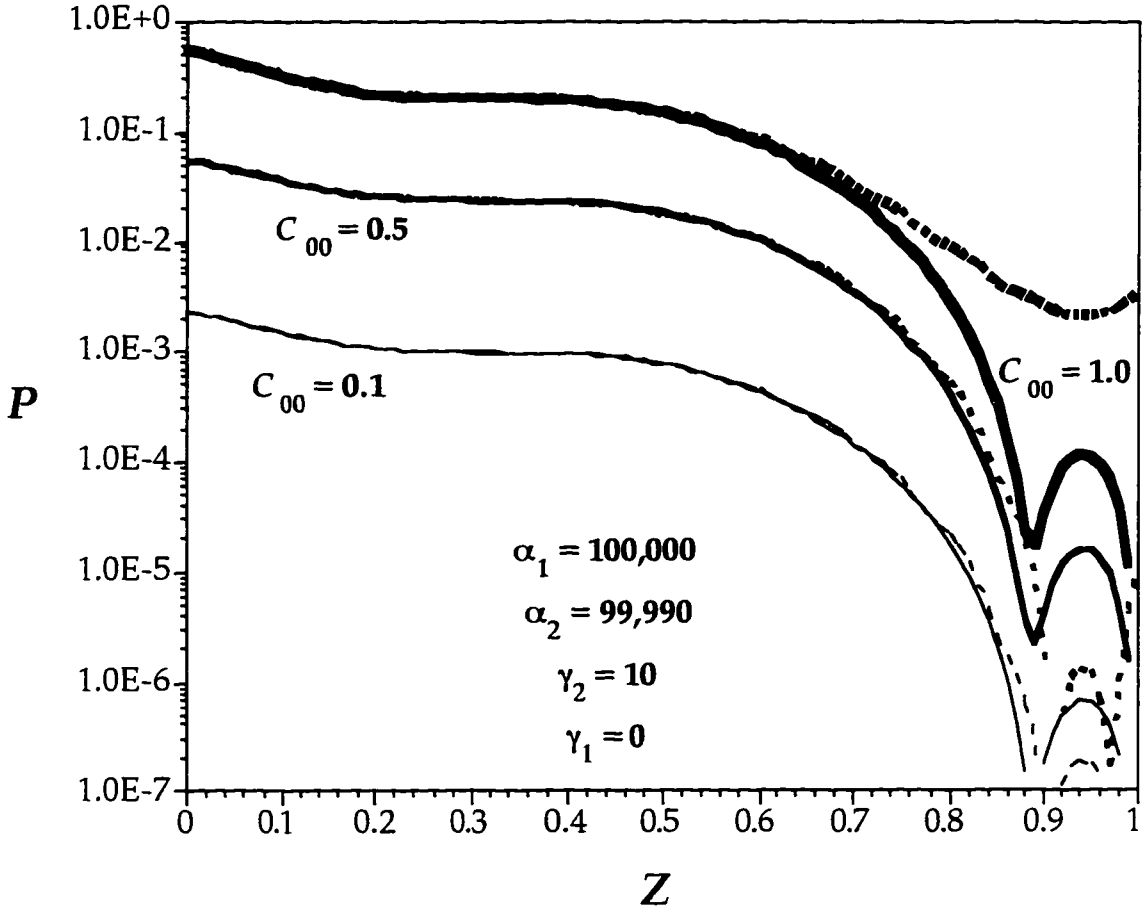

Figure 13. Comparison between numerical (dashed lines) and approximate (solid lines) solutions for an optical fiber with two co-located Bragg gratings (α_1=100,000, α_2=99,950, γ_1=0, γ_2=10 and C_{00}=0.1, C_{00}=5 and C_{00}=7).

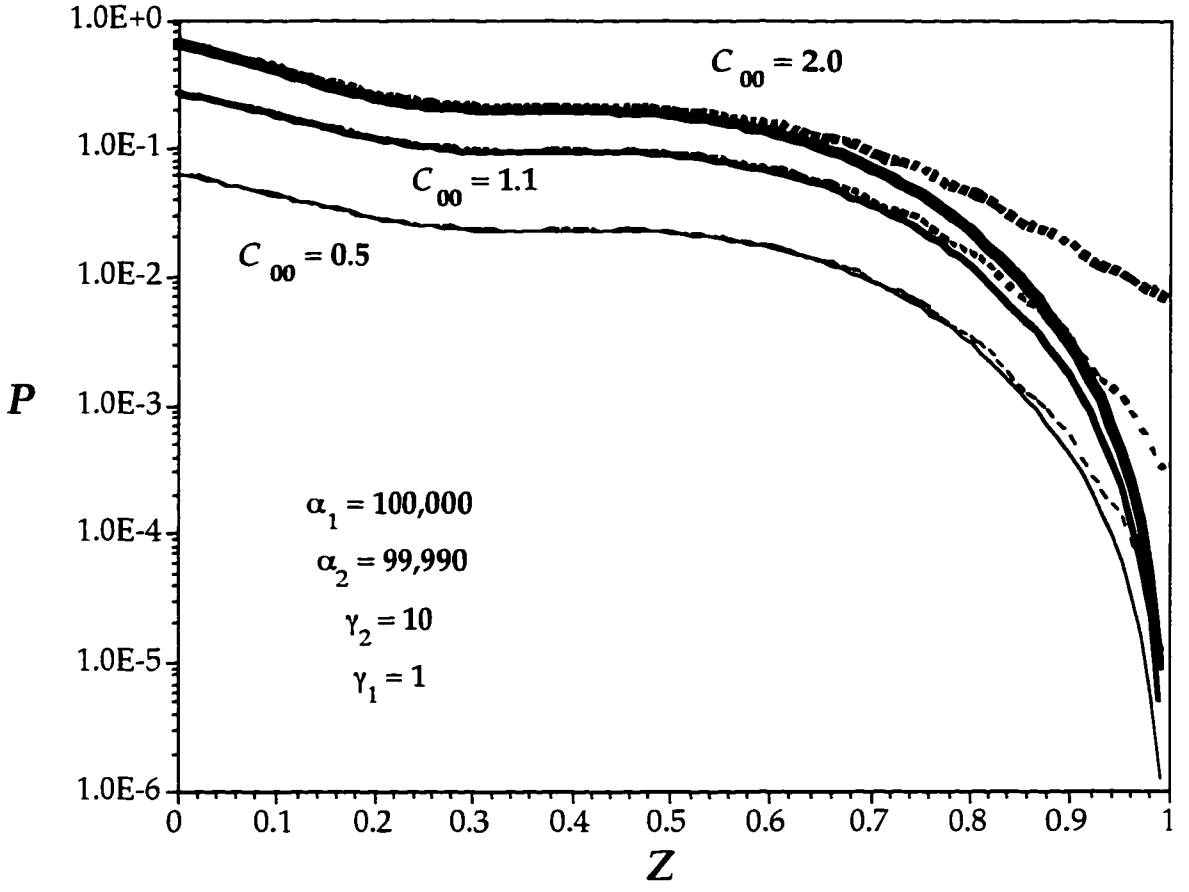

Figure 14. Comparison between numerical (dashed lines) and approximate (solid lines) solutions for an optical fiber with two co-located Bragg gratings (α_1=100,000, α_2=99,950, γ_1=1, γ_2=10 and C_{00}=0.5, C_{00}=1.1 and C_{00}=2).

Z; an effect due to the presence of the second grating. As it was discussed before, the departure from the approximate solution might be due to the possibility that the numerical solution diverges at these values of Z. This explanation seems adequate because of the matching between the two solutions at low to moderate Z-values.

The comparison discussed in the previous paragraph, is evidence that the approximations derived work fairly well within a large interval of values, specially at low values of the coupling constant. Taking that into account, the reflectivity was determined for the two Bragg grating fiber and plotted in Figs. 15 and 16 against the two normalized phase matching variables, γ_1 and γ_2. The value used for the normalized coupling constant was the unity whereas the value chosen for α_1 was 100,000. As it can be seen, Figs. 15 and 16 are contour plots of the reflectivity with the contour lines spaced by 2%. The maximum value of the reflectivity occurs nearby the center of both graphs, around $\gamma_1=0$. In this region, there are several lobes aligned *almost parallel* to the γ_2 axis; it is inside these lobes that the maximum value of the reflectivity occurs. Notice that the higher the modulus of γ_2, the closer the center of the lobes are to $\gamma_1=0$, i.e., the higher the modulus of γ_2, the closer the first order and asymptotic solutions are to each other. However, the lower the modulus of γ_2, the more the peak reflectivity deviates from the phase matching condition $\gamma_1=0$. In other words, *a lower value of γ_2 displaces the phase matching condition of the first grating*, i.e., lower values of γ_2 leads to a phase matching condition in the first grating in which $\gamma_1\neq0$. *This displacement in the phase matching condition leads to a shift in the Bragg wavelength of the first grating.*

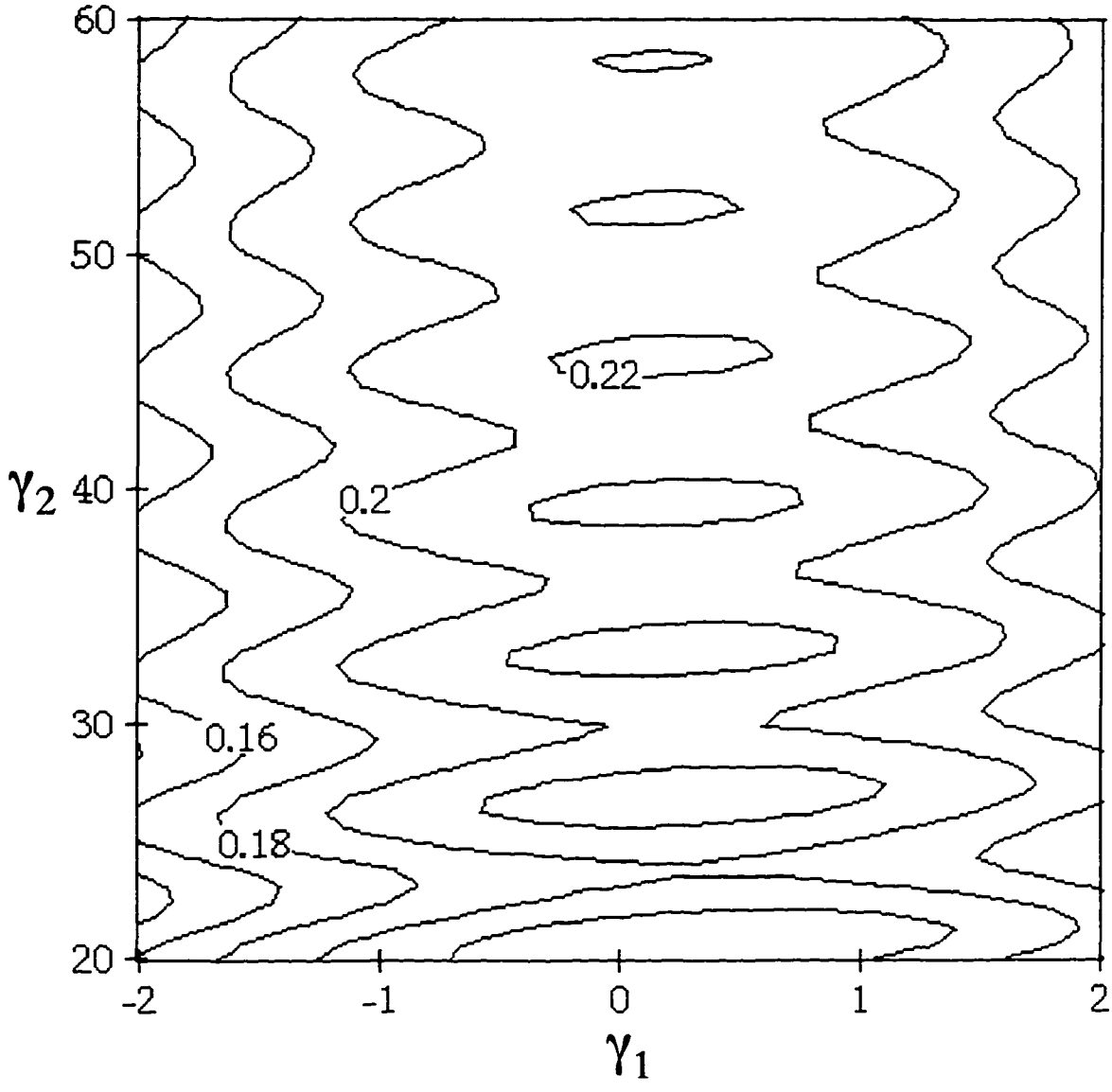

Figure 15. Contour plot of the reflectivity against the two normalized phase matching parameters of a dual Bragg grating optical fiber for $C_{00}=1$ ($\gamma_2>0$).

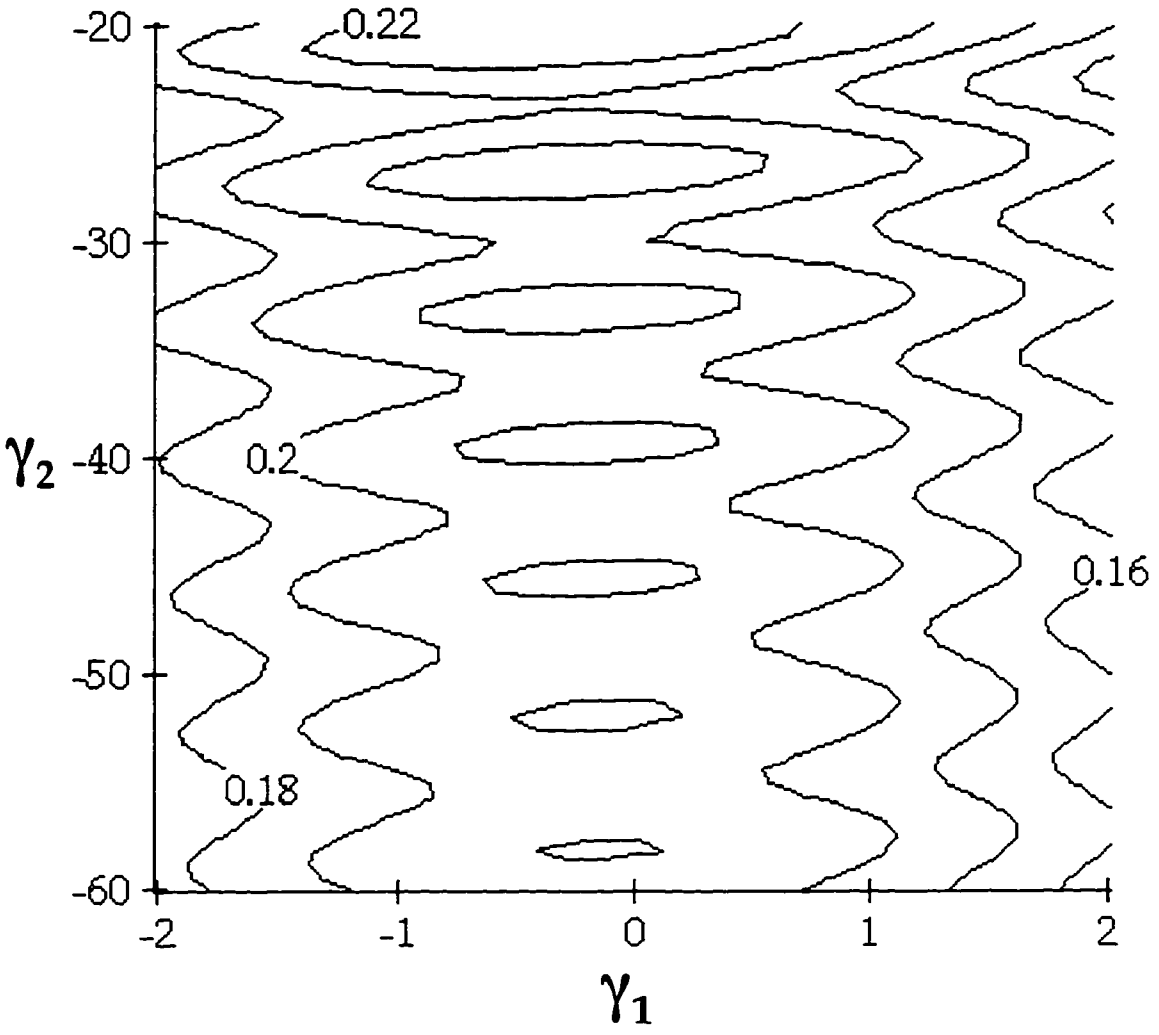

Figure 16. Contour plot of the reflectivity against the two normalized phase matching parameters of a dual Bragg grating optical fiber for $C_{00}=1$ ($\gamma_2<0$).

Whereas for the single Bragg grating the peak reflectivity occurs at $\gamma_1=0$, for the double Bragg grating , the peak reflectivity may occur at $\gamma_1\neq 0$, unless $|\gamma_2|$, is very large and the first order correction can be neglected. It is noted that a lower $|\gamma_2|$, means Ω_2 closer to Ω_1. Obviously, the equations derived fails whenever Ω_2 gets infinitely closer to Ω_1 due to the fact that the equations were derived for $|\gamma_2|>10$.

Another result that follows from Figs. 15 and 16 is the following; *negative (positive) values of γ_2 shifts the peak reflectivity of the first grating towards negative (positive) values of γ_1*. Rephrasing the above; positive values of γ_2 shifts the center of the lobes in the reflectivity plot towards positive values of γ_1 (see Fig. 15) whereas negative values of γ_2 shifts the center of the lobes towards negative values of γ_1 (see Fig. 16).

The shift direction in the wavelength space can be easily derived from the above results. The Bragg wavelength, $\lambda_{1,B}$, for a single Bragg grating fiber with frequency Ω_1 can be written as ($\gamma_{1,B}=0$)

$$\lambda_{1,B}=\frac{4\pi n_{eff}}{\Omega_1}. \tag{51}$$

Whenever a second Bragg grating is introduced with $\gamma_2<0$, i.e., $\Omega_2>\Omega_1$, the Bragg condition of the first grating is shifted towards negative values of the normalized phase matching parameter or $\gamma_{1,B}<0$. This leads to a final Bragg wavelength, $\lambda'_{1,B}$, given by

$$\frac{4\pi n_{eff}}{\lambda'_{1,B}} - \Omega_1 < 0$$

or

$$\lambda'_{1,B} > \lambda_{1,B}.$$

So, for $\Omega_2 > \Omega_1$, $\lambda'_{1,B} > \lambda_{1,B}$ whereas the converse is also true.

V.4 Estimate of the shift in wavelength due to a second Bragg grating

A quick estimate of the amount of shifting in the first Bragg wavelength, due to the addition of a second one, can be made by knowing the Bragg value of γ_1 after the second grating is written. Assuming that this value is $\gamma_1 \cong 1$, the final Bragg wavelength will be given by

$$\frac{4\pi n_{eff}}{\lambda'_{1,B}} = \Omega_1 + \frac{1}{L}$$

where n_{eff} is the effective index of refraction given by

$$n_{eff} = \frac{\beta}{k}.$$

The shifted wavelength can then be determined as

$$\lambda'_{1,B} = \frac{4\pi n_{eff}}{\Omega_1 + \frac{1}{L}}. \qquad (52)$$

The effective refractive index has a value within the interval $n_{core} > n_{eff} > n_{clad}$ which, for a weakly guiding optical fiber made of silica, leads to values that fall within the interval $1.46 > n_{eff} > 1.45$. Let the length of the Bragg grating L be $L = 0.03m$ and the initial Bragg wavelength of the first grating around $\lambda_{1,B} = 1.3\mu m$. At this initial Bragg wavelength, the frequency Ω_1 is roughly $14.1 \times 10^6 m^{-1}$. Using these values into Eq. (52), the final wavelength turns out to be $\lambda'_{1,B} = 1.301\mu m$, or one nanometer longer than the initial value.

As it can be seen a second Bragg grating may shift the Bragg wavelength of a fibers grating by roughly $1nm$. The direction of shift depends on the signal of the normalized phase matching parameter of the second grating, i.e., positive values of γ_2 shifts the Bragg wavelength of the first grating towards lower values whereas negative values of γ_2 shifts the Bragg wavelength towards higher values. Indeed such an effect has been observed before by Othonos et al. [1994]. In their experiment, a shift of almost $1nm$ was observed whenever six additional gratings were written over the a first one. The authors attributed the shift to a variation in the effective index of refraction. Here it is proposed that this variation results from the inscription of a additional gratings.

CHAPTER VI

APPLICATIONS OF THE OPTICAL FIBER BRAGG GRATING SOLUTION TO OTHER DEVICES

VI.1 Introduction

In this Chapter, three different applications of an optical fiber Bragg grating are explored; they involve coupling among modes without azimuthal symmetry such as in a two mode fiber, coupling within a four mode fiber and the effect of the axial strain and temperature in the shift of the Bragg wavelength.

VI.2 Coupled Equations for a two Mode Fiber

The coupled equations of a two mode fiber can be derived directly from Eqs. (1) and (2) for $N=2$ or

$$\frac{dc_0^{(+)}}{dz} = \left(c_1^{(-)} e^{(\beta_1+\beta_0)iz} + c_1^{(+)} e^{(\beta_0-\beta_1)iz}\right) k_{01} + \left(c_0^{(+)} + c_0^{(-)} e^{2\beta_0 iz}\right) k_{00} \tag{53}$$

$$\frac{dc_0^{(-)}}{dz} = -\left(c_1^{(+)} e^{-(\beta_1+\beta_0)iz} + c_1^{(-)} e^{(\beta_1-\beta_0)iz}\right) k_{01} - \left(c_0^{(-)} + c_0^{(+)} e^{-2\beta_0 iz}\right) k_{00} \tag{54}$$

$$\frac{dc_1^{(+)}}{dz} = \left(c_1^{(+)} + c_1^{(-)} e^{2\beta_1 iz}\right) k_{11} + \left(c_0^{(-)} e^{(\beta_1+\beta_0)iz} + c_0^{(+)} e^{(\beta_1-\beta_0)iz}\right) k_{10} \tag{55}$$

and

$$\frac{dc_1^{(-)}}{dz} = -\left(c_1^{(-)} + c_1^{(+)} e^{-2\beta_1 iz}\right) k_{11} - \left(c_0^{(+)} e^{-(\beta_1+\beta_0)iz} + c_0^{(-)} e^{(\beta_0-\beta_1)iz}\right) k_{10} \tag{56}$$

As it can be seen, from Eqs. (53) through (56), there are four coupling constants associated with them namely, k_{00}, k_{11}, k_{01} and k_{10}, where the numerals "0" and "1" stand for the fundamental and LP_{11} modes. These coupling constants are given by Eq. (3) and can be written as

$$k_{00} = \frac{\omega \varepsilon_0 i}{4P} \int_0^{2\pi} \int_0^{\infty} \left(n_0^2 - n^2\right) \left|E_{t,0}\right|^2 r\, dr\, d\phi \tag{57}$$

$$k_{11} = \frac{\omega \varepsilon_0 i}{4P} \int_0^{2\pi} \int_0^{\infty} \left(n_0^2 - n^2\right) \left|E_{t,1}\right|^2 r\, dr\, d\phi \tag{58}$$

$$k_{01} = \frac{\omega \varepsilon_0 i}{4P} \int_0^{2\pi} \int_0^{\infty} \left(n_0^2 - n^2\right) E_{t,1} E_{t,0}^{*} r\, dr\, d\phi \tag{59}$$

and

$$k_{10} = \frac{\omega \varepsilon_0 i}{4P} \int_0^{2\pi} \int_0^{\infty} (n_0^2 - n^2) E_{t,0} E_{t,1}^* \, r \, dr \, d\phi \quad . \qquad (60)$$

Whenever, the refractive index variation along the fiber has azimuthal symmetry, such as in the case of a Bragg grating perpendicular to the fiber axis [see Eq. (6)], $n \neq n(\phi)$ and Eqs. (59) and (60) are zero because of the orthogonality relation between two modes of different order. In this case there is no coupling between the LP_{01} and LP_{lm} modes for $l \neq 0$ and coupling occurs only between the forward and backward propagating modes.

However, whenever the azimuthal symmetry is broken, an additional ϕ dependency is introduced in the integration of the azimuthal variable ϕ and the final result may be different of zero. Such is the case of a tilted or blazed Bragg grating in which the refractive index can be written as

$$n = n_0 + \delta n \cos(z' \Omega) \qquad (61)$$

where z' is the axis along the *tilted* Bragg grating which is assumed to make an angle δ with the fiber axis (see Fig. 17). The tilted z'-axis can then be written as

$$z' = y \sin(\delta) + z \cos(\delta) \qquad (62)$$

where

$$y = r \sin(\phi) \cdot \tag{63}$$

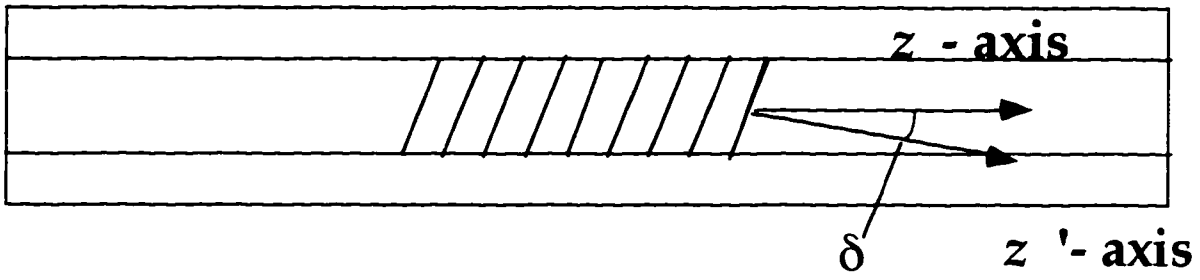

Figure 17. Optical fiber with a blazed Bragg grating.

By introducing Eqs. (61) through (63) into (59) and (60), it can be easily seen that the tilted Bragg grating introduces a ϕ dependence that works towards to make Eqs. (59) and (60) different of zero.

VI.3 Conditions for Coupling Among Modes in a Four Mode Fiber

Mode conversion in a four mode fiber has been experimentally observed by Bilodeau et al. [1991]. Subsequent work by Shi and Okoshi [1992] has analysed the conversion characteristics between the LP_{01} and LP_{02} modes only. Here the coupled mode equations are used to determine the characteristics of coupling among all modes involved. The starting point again are Eqs. (1) and (2) for N=4. Assuming that only the forward fundamental mode is excited initially, coupling will occur only between the forward and backward fundamental and LP_{02} modes.

The conditions for each of these couplings are obtained directly from the coupled mode equations using the phase matching condition in the argument of the exponentials associated with the two modes. For instance, the condition for coupling between the forward and backward fundamental mode is obtained from the differential equation that contains the derivative $dc_0^{(+)}/dZ$. The phase matching condition is the one derived from the argument of the exponential that comes along with the $c_0^{(-)}$ or

$$\gamma_0 = 0.$$

The above condition leads to

$$\Omega = 2\beta_{01} \tag{64}$$

which is the condition for maximum power transfer between the forward and backward propagating fundamental modes. Let

$$\Omega = 2\frac{\pi}{\Lambda},$$

where Λ is period of the grating, then the phase matching condition in Eq. (64) reduces to

$$\Lambda = \frac{\pi}{\beta_{01}}.$$

Doing the same for the other two cases, it is obtained

$$\Lambda = \frac{2\pi}{\beta_{02} + \beta_{01}}$$

for coupling between the forward fundamental and backward LP_{02} and

$$\Lambda = \frac{2\pi}{\beta_{01} - \beta_{02}}$$

for the forward fundamental and forward LP_{02}.

As it can be seen there are three different conditions for phase matching for each mode; each of these conditions are a function of the grating period and the propagation constant of the modes. If a given grating period is chosen such that the propagation constant of the fundamental mode is maximum at λ=1.3μm, i.e., $\beta_{01}=k\,n_{core}$, with n_{core}=1.46, the grating period will be given by

$$\Lambda = 4.45\text{x}10^{-7}\ m\ . \qquad (65)$$

Assuming that the propagation constant of the LP_{02} is $k\,n_{clad}$, with n_{clad}=1.45, the Bragg wavelength, for coupling between the forward fundamental and backward LP_{02} will be at

$$\lambda_{0\text{-}3} = 1.296\text{x}10^{-6}\,m$$

As it can be seen, the difference between these two Bragg wavelengths is almost 4.5nm and, as such, it should be possible to distinguish these two

Bragg wavelengths by scanning the reflectivity spectrum of a Bragg grating fiber with a spectrum analyser. Indeed, a more general estimate predicts that the difference between the Bragg wavelengths of these two modes is on the order of

$$|\lambda_{0-3} - \lambda_{00}| = \frac{(n_{\text{core}} - n_{\text{clad}})\,\lambda_{00}}{2\,n_{\text{core}}},$$

i.e., the longer the period of the grating, the larger the difference between the Bragg wavelengths. However, it should be pointed out that these values are just an upper limit.

For the case of coupling between the forward fundamental and forward LP_{02} using the grating period given by Eq. (65), the Bragg wavelength would be very short, on the order of 4 nm, and way outside the visible spectrum. So, for coupling between these two modes to occur, the grating period must be much longer than the one in Eq. (65).

VI.4 Effects of Temperature and Axial Strain in the Bragg Wavelength

Bragg grating optical fibers can be used as strain temperature sensors. The principle used consists in monitoring the shift in the Bragg wavelength due to mechanical and thermal strain. The Bragg wavelength can be determined from the following Equation

$$\lambda_B = 2\,n_{\text{eff}}\,\Lambda \qquad (66)$$

where both the effective refractive index n_{eff} and the grating period changes as mechanical and thermal strain are applied or

$$\delta\lambda_B = 2\left(\delta n_{eff}\,\Lambda + n_{eff}\,\delta\Lambda\right).$$

Equation (66) is very similar to the expression for the phase of a Mach-Zender optical fiber configuration [Butter and Hocker, 1978; Hocker, 1979; Sirkis and Haslach, 1991 and Egalon and Rogowski, 1991; 1992a; 1992b; 1992c and 1994] which is given by

$$\phi = \beta L \tag{67}$$

where L is the length of the fiber that is undergoing strain. Comparing Eqs. (66) and (67), it can be easily realized that L corresponds to Λ, the grating period, whereas β, corresponds to n_{eff}. Indeed these two expression are proportional to each other. For this reason, the expression of the shift in the Bragg wavelength is the same as the one for phase shift of a Mach-Zender sensor less a constant. Based on this identification, the shift in the Bragg wavelength due to axial strain, for an optical fiber that is surface mounted, can be easily written in terms of previous results found in the literature or, for a shift due to mechanical strain [Butter and Hocker, 1978; Sirkis and Haslach, 1991 and Egalon and Rogowski, 1991; 1992a; 1992b and 1994]

$$\delta\lambda_{B,M} = 2n_{core}\left[1 - n_{core}^2\,P_{ef} + \Delta\frac{U_{ln}^2}{V^2}\left(n_{core}^2\left(3 - 4\eta_{ln}\right)P_{ef} - 1 - 2\mu\eta_{ln}\right)\right]\Lambda\,\varepsilon \tag{68}$$

where

$$P_{ef} = \frac{[p_{12} - (p_{12} + p_{11})\,\mu]}{2} \quad , \tag{69}$$

$$\eta_{ln} = \frac{K_l^2(W_{ln})}{K_{l+1}(W_{ln})K_{l-1}(W_{ln})} \quad , \tag{70}$$

$$W_{ln} = \sqrt{V^2 - U_{ln}^2} \quad , \tag{71}$$

$$\Delta = \frac{n_{\text{core}}^2 - n_{\text{clad}}^2}{2n_{\text{core}}^2} \, , \tag{72}$$

p_{11} and p_{12} are components of the strain optic tensor, ε the value of the axial strain, μ the Poisson's ratio for the fiber, K_l the modified Bessel function of order l and W_{ln} and U_{ln} the eigenvalues of a mode of a weakly guiding fiber of order l and rank n. It can be easily shown that the term in Δ contributes less than 1% to the total shift in the Bragg wavelength [Egalon and Rogowski, 1992b and 1994], for this reason Eq. (68) can be simplified to

$$\delta\lambda_{B,M} \cong 2n_{\text{core}}\left(1 - P_{ef}\, n_{\text{core}}^2\right) \Lambda\, \varepsilon \quad . \tag{73}$$

As it can be seen from the above, sensitivity of the sensor increases with the Bragg period and decreases with the effective strain optic coefficient, P_{ef}.

Doing the same for the effect of temperature, the shift in the Bragg

wavelength can be written as [Hocker, 1979; Sirkis and Haslach, 1991 and Egalon and Rogowski, 1992c]

$$\delta\lambda_{B,T} = 2\left[\frac{dn}{dT} + \alpha n_{\text{core}} + \Delta\frac{U_{ln}^2}{V^2}\left(\eta_{ln}\left(\frac{dn}{dT} + 2\alpha n_{\text{core}}\right) - \alpha n_{\text{core}}\right)\right]\Lambda\,\delta T \tag{74}$$

where δT is the variation in from a set point and α and dn/dT are the thermal expansion coefficient and the thermal refractive coefficient of the fiber. Again Eq. (74) can be simplified to

$$\delta\lambda_{B,T} = 2\left[\frac{dn}{dT} + \alpha n_{\text{core}}\right]\Lambda\,\delta T \quad . \tag{75}$$

As before, sensitivity increases with the grating period.

The condition for a Bragg grating optical fiber strain sensor insensitive to axial strain is exactly the same as the one for a strain insensitive Mach-Zender sensor [Egalon and Rogowski, 1992b and 1994] or

$$n_{\text{core}} = \frac{1}{\sqrt{P_{\text{ef}}}} \tag{76}$$

whereas for a temperature insensitive fiber the condition is

$$n_{\text{core}} = -\frac{1}{\alpha}\frac{dn}{dT} \quad . \tag{77}$$

Using values that are typical for a silica fiber (n_{core}=1.46 and P_{ef}=0.102) and a grating period consistent with a peak at λ=1550 nm, or Λ=5.31 10^{-7} m, the shift in the wavelength due to mechanical strain is

$$\delta\lambda_{B,M} = 1.02\ 10^{-6}\ \varepsilon\ m \quad . \tag{78}$$

For ε=750 μ-strain the above relation reduces to $\delta\lambda_B$=0.765 nm, which is roughly the value 0.8 nm obtained by Kersey and Morey [1993]. For higher strain values, such as 10,000 μ-strain, which is the breaking point of silica, the shift can be as large as 10 nm.

The mechanical and temperature strain formulas have been compared with another experimental result [Xu et al., 1994]. Table 2 summarizes these results. Within the range of 0-600 μ-strain, and at Bragg wavelengths of 1300 nm and 850 nm the relations for the wavelength shift and strain obtained by Xu et al. [1994] were found to be 0.96x10^{-6} ε m and 0.59x10^{-6} ε m, respectively. Using Eq. (78), the relations obtained are 0.855 x 10^{-6} ε m at 1300 nm and 0.56 x 10^{-6} ε m at 850 nm; a difference of less than 10%.

For thermal strain within the temperature range 10 and 60°C, Xu et al. [1994], found slope values of 8.72x10^{-12} m /°C and 6.3 x 10^{-12} m /°C, at 1300 and 850 nm, respectively. Using the thermal constants of a silica fiber given by [Hocker, 1978], α=5x10^{-7}/°C and dn /dT=10^{-5}/°C, these slopes are 9.575x$10^{-12}$$m$ /°C and 6.26x10^{-12} m /°C, again a difference of less than 10%.

For the case of a temperature variation between –273°C and 800°C and $\alpha=5\text{x}10^{-7}/^{\circ}\text{C}$ and $dn/dT=10^{-5}/^{\circ}\text{C}$, which are values for the silica fiber [Hocker, 1978], the shift in the Bragg wavelength for a grating period of 1300 nm, is 5.1 nm.

Table 2. Slope values for the shift of the Bragg wavelength at 1300 and 850 nm, for mechanical and thermal strain. Experimental values are from Xu et al. [1994] whereas theoretical values are from Equations (73) and (75). Parameters used are for a silica fiber.

strain	wavelength (m)	Experimental [Xu et al., 1994]	Theory
mechanical	1300	$0.96\text{x}10^{-6}m$	$0.855\text{x}10^{-6}m$
	850	$0.59\text{x}10^{-6}m$	$0.56\text{x}10^{-6}m$
thermal	1300	$8.72\text{x}10^{-12}m$ /°C	$9.58\text{x}10^{-12}m$ /°C
	850	$6.3\text{x}10^{-12}m$ /°C	$6.26\text{x}10^{-12}m$ /°C

CHAPTER VII

CONCLUSIONS

The asymptotic solution of a single Bragg grating optical fiber was reformulated. A first order correction has been determined using the Method of the Successive Approximations. Using these results, a solution for a two Bragg grating optical fiber was determined. It was found that a second Bragg grating shifts the Bragg wavelength of the first one by a small amount. This shift is towards longer (shorter) wavelengths whenever the period of the second grating is smaller (greater) than the period of the first one. The shift increases whenever the Bragg wavelength of the second grating is closer to the Bragg wavelength of the first one. A similar shift, in which multiple Bragg gratings were written in a fiber, has also been reported in the literature [Othonos et al., 1994].

A theoretical analysis of a Bragg grating optical fiber with two and four modes was presented. It has been shown that a tilted Bragg grating is capable of coupling light into modes of different orders by introducing a non-zero coupling constant. Results of two co-propagating modes using the coupled mode equations have been compared with work published elsewhere [Snyder and Davis, 1978]. It has been found that the numerical solution does not match the approximate solution derived by Snyder and Davis [1978]. Furthermore, coupling within a four modes optical fiber has also been investigated. It was shown that coupling between two forward propagating

modes occurs for grating periods much longer than the period required for coupling between a forward and backward propagating modes. This indicates that coupling between two forward propagating modes is much more sensitive to axial and thermal strain.

Finally, relations for the shift in the Bragg wavelength due to thermal and mechanical strain have been derived. These relations were compared with experimental results and it was found that the agreement is within 10%.

The procedure outlined here can be applied to model other devices which use modal coupling such as tapered couplers, distributed feedback lasers, optical fiber filters and sensors.

LIST OF REFERENCES

3M Corporation, "3M Single-Mode Fiber Products", Introduction to Fiber Bragg Gratings, 1996.

R.Allen, L.Esterowitz, "CW diode pumped 2.3 μm fiber laser", *Appl. Phys. Lett.*, Vol. 55, No. 8, pp. 721-722, 1989.

C. G. Askins et al., "Fiber Bragg reflectors prepared by a single excimer pulse", *Opt.Lett.*, Vol. 29, pp. 1668-1669, 1993.

A. Asseh, H. Storoy, J. T. Kringlebotn, W. Margulis, B. Sahlgren, S. Sandgren, R. Stubbe and G. Edwall, "10 cm Yb^{3+} DFB fibre laser with permanent phase shifted grating", *Elect. Lett.*, Vol. 31, No. 12, pp. 969-970, June 1995.

G. A. Ball and W. W. Morey, "Continously tunable single-mode erbium fiber laser", Optics Letters, Vol. 17, No. 6, pp. 420-422, March 1992.

F. Bilodeau, K. O.Hill, B. Malo, D. C. Johnson and I. M. Skinner, "Efficient, narrowband LP01↔LP02 mode convertors fabricated in photosensitive fibre: spectral response", *Elect. Letters*, Vol. 27, No. 8, pp. 682-684, April 1991.

J. N. Blake, B. Y. Kim, H. J. Shaw, "Fiber-optic modal coupler using periodic microbending", *Opt. Lett.*, vol. 11, pp. 177-179, 1986.

M. C. Brierley, P. W. France, C. A. Millar, "Lasing at 2.08 μm and 1.38 μm in a holmium doped fluorozirconate fibre laser", *Ellect. Lett.* , Vol. 24, No. 9, pp. 539-540, 1988.

D. A. Cardimona, M. P. Sharma, V. Kovanis and A. Gavrielides, "Dephased Index and Gain Coupling in Distributed Feedback Lasers", IEEE J. Quantum Electronics, Vol., 31 No. 1, pp. 60-66, January 1995.

L. Dong et al., "Single pulse Bragg gratings written during fibre drawing", *Electr. Lett.*, Vol. 29, pp. 1577-1578, 1993.

C. O. Egalon, A. M. Buoncristiani and R. S. Rogowski, "Analytical approximation and first order correction of the coupled mode equations", submitted for publication to Optical Engineering, 1996.

C. O. Egalon and R. S. Rogowski, "Model of an Axially Strained Weakly Guiding Optical Fiber Modal Pattern", Fiber Optic Smart Structures and Skins IV, Proceedings of SPIE, Vol. 1588, pp. 241-254, September 1991.

C. O. Egalon and R. S. Rogowski, "Model of an Axially Strained Weakly Guiding Optical Fiber Modal Pattern", *Optical Engineering*, Vol. 31, No. 6, pp. 1332-1339, June 1992a.

C. O. Egalon and R. S. Rogowski, "Axial strain insensitivity of weakly guiding optical fibers ", Proceedings of OE FIBER'92, SPIE, vol. 1798, pp. 42-47, October 1992b.

C. O. Egalon and R. S. Rogowski, "Temperature effects in the modal phase shift of a weakly guiding fiber", Proceedings of OE FIBER'92, SPIE, vol. 1798, pp. 167-174, October 1992c.

C. O. Egalon and R. S. Rogowski,"Axial strain insensitivity of weakly guiding optical fibers",*Optical Engineering*, Vol. 33, No. 2, pp. 498-501, February 1994.

L. Esterowitz, R. allen; I. Aggarwal, "Pulsed laser emission at 2.3μm in a thulium-doped fluorozirconate fibre", *Ellect. Lett.*, Vol. 24, No. 17, pp. 1104, August 1988.

M. C. Farries, P. R. Morkel, J.E. Townsend, "The properties of the samarium fibre laser", *Fiber Laser Sources and Amplifiers*, Proc. SPIE, Vol. 1171, pp. 271-278, 1989.

D. Greenspan, "Theory and solutions of ordinary differential equations", The Macmillan Company, New York, N. Y., 1960.

D. C. Hanna, R. M. Percival, R. G. Smart, J. E. Townsend, A.C. Tropper, "Continuous wave oscillation of holmium-doped silica fibre laser", *Ellect. Lett.*, Vol. 25, No. 9, pp. 593-594, 1989.

D. C. Hanna, R. M. Percival, I. R. Perry, R. G.Smart, P. J. Sunni, J. E. Townsend, A.C. Tropper, "Continuous wave oscillation of a monomode ytterbium-doped fibre laser", *Ellect. Lett.*, Vol. 24, No. 17, pp. 1111-1113, 1988.

H. A. Haus and W. Huang, "Coupled mode theory", Proceedings of the IEEE, vol. 79, no. 10, pp. 1505-1518, October 1991.

K. O. Hill, B.Malo, K.A. Vineberg, F. Bilodeau, D. C. Johnson and I. Skinner, "Efficient mode conversion in telecommunication fiber using externally written gratings", *Electron. Lett.*, Vol. 26, pp. 1270-1272, 1990.

K.O. Hill et al., "Bragg gratings fabricated in monomode photosensitive optical fiber by UV exposure through a phase mask", *Appl. PHys. Lett.* vol. 62, pp. 1035-1037, 1993.

G. B. Hocker, "Fiber-optic sensing of pressure and temperature", *Appl. Opt*, Vol. 18, No. 9, pp. 1445-1448, 1979.

W. P. Huang, B. E. Little and C. L. Xu, "On phase matching and power coupling in grating-assisted couplers", IEEE Photon. Tech. Letters, Vol. 4, No. 2, pp. 151-153, February 1992.

E. L. Ince, "Ordinary Differential Equations", Dover, New York, N. Y., 1956.

A. D. Kersey and W. W. Morey, "Multiplexed Bragg grating fibre-laser strain-sensor system with mode-locked interrogation", *Elect. Lett.*, Vol. 29, No. 1, January 1993.

H. Kogelnik and C. V. Shank, "Coupled wave theory of distributed feedback lasers", J. Appl. Phys., vol. 43, no. 5, pp. 2327-2335, May 1972.

D.K. Lam and B.K. Garside, "Characterization of single-mode optical fiber filters", Applied Optics, Vol. 20, No. 3, pp. 440-445, February 1981.

C.M. Lawrence, D. V. Nelson and E. Udd, "Multi-parameter sensing with fiber Bragg gratings", to published, 1996.

H. G. Limberger, P. Y. Fonjallaz and R. P. Salathé, "Spectral characterization of photoinduced high efficient Bragg gratings in standard telecommunication fibres", *Elect. Lett.*, Vol. 29, No. 1, January 1993.

D. Marcuse, "Coupled mode theory of round optical fibers", The Bell System Technical Journal, Vol. 52, No. 6, pp. 817, 1973.

D. Marcuse, Theory of Dielectric Optical Waveguides, Academic Press, New York, N.Y., 1974.

D. Marcuse, "Light Transmission Optics", van Nostrand Reinhold Company, New York, N.Y., 1982,

D. Marcuse, "DFB laser with attached external intensity modulator", IEEE Jorn. Quantum Electronics, vol. 26 no. 2, pp. 262-269, February 1990.

M. J. Maron, "Numerical Analysis: a Practical Approach", Macmillan Publishing Co., Inc., New York, 1982.

R. J. Mears, L. Reekie, I. M. Juancey and D. N. Payne, "Low-noise erbium-doped fibre amplifier operating at 1.54 μm", *Elect. Letters*, Vol. 23, No. 19, pp. 1026-1028, September 1987.

G. Meltz, W. W. Morey and W. H. Glenn, "Formation of Bragg gratings in optical fibers by a transverse holographic method", Opt. Lett. Vol. 14, No. 15, pp. 823-825, 1989.

S. E. Miller, "On solutions for two waves with period coupling", The Bell System Technical Journal, vol. 48, pp. 1801-1822, October 1968.

W. W. Morey, G. Meltz and W. H. Glenn, "Fiber optic Bragg grating sensors", SPIE Proceedings, Vol. 1169, Fiber Optic and Laser Sensors VII, pp. 98-106, 1989.

W. W. Morey, G. A. Ball and G. Meltz, "Photoinduced Bragg grating in optical fibers", Optics & Photonics News, vol. 5, no. 2, pp. 8-14, February 1994.

Y. Ohishi, T. Kanamori, T. Kitagawa, S. Takahashi, E. Snitzer, G. H. Sigel, Jr, "Pr^{3+}-doped fluoride fiber amplifier operating at 1.31 μm ",*Optical Fiber Communication Conference Technical Digest*, OSA, pp. 10-13, 1991.

A. Othonos, X. Lee and R.M. Measures, "Superimposed multiple Bragg gratings", *Ellect. Lett.*, vol. 30, No. 23, pp. 1972-1974, November 1994.

H. G. Park, S. Y. Huang and B. Y. Kim, "All-optical intermodal switch using periodic coupling in a two-mode waveguide", Optics Letters, vol. 14, no.16, pp. 877-879, August 1989.

H. G. Park and B. Y. Kim, "Intermodal coupler using permanently photoinduced grating in two-mode optical fiber", *Electron. Lett.*, Vol., 25, pp. 797-799, 1989.

R. M. Percival, M. W. Phillips, D. C. Hann, A. C. Tropper, "Characterization of spontaneous and stimulated emission from praseodymium (Pr^{3+}) ions doped into a silica-based monomode optical fiber", *IEEE J. Quant. Elect.*, Vol. 25. No. 10, pp. 2119-2123, 1989.

Prescience Corporation, "Theorist Reference Manual", version 2.00, San Francisco, CA, 1994.

L. Reekie, R. J. Mears, S. B. Poole and D. N. Payne, "Tunable single-mode fiber lasers", *J. Light. Tech.*, Vol. LT-4, No. 7, pp. 956-960, July 1986.

H. E. Rowe, "Approximate solutions for the coupled line equations", The Bell System Technical Journal, vol. , pp.1011-1029, May 1962.

M. Sejka, P.Varming, J. Hubner and M. Kristensen, "Distributed feedback Er^{3+}-doped fibre laser", *Elect. Letters*, vol. 31, No. 17, pp. 1445-1446, August 1995.

C-X Shi and T. Okoshi, "Analysis of a fiber-optic $LP_{01} \leftrightarrow LP_{02}$ mode converter", Optics Letters, Vol. 17, No. 10, pp. 719-721, May 1992a.

C-X Shi and T. Okoshi, "Mode conversion based on the periodic coupling by a reflective fiber grating", Optics Letters, Vol. 17, No. 23, pp. 1655-1657, December 1992b.

Sirkis, J.S. and Haslach Jr.,H.W. "Complete Phase-Strain Model for Structurally Embedded Interferometric Optical Fiber Sensors", *Journal of Intelligent Material Systems and Structures*, Vol 2, No. 1, pp. 3-24, January 1991.

A. W. Snyder, and W. J. Davies, "Assymptotic solution of coupled mode equations for sinusoidal coupling", Proceedings of the IEEE, pp. 168-169, January 1970.

A.W. Snyder, and J. D. Love, Optical Waveguide Theory, Chapman and Hall, New York, N.Y., 1983.

E. Udd, "Advanced strain measurement applications of fiber optic grating sensors", o be published, 1996.

V. A. Volpert and Vl. A. Volpert, "Determination of the combustion wave velocity asymptotics by the successive approximation method", Zhurnal Prikladnoi Mekhaniki i Tekhnichesskoi Fiziki, pp. 19-26, September-October 1990.

A. Yariv, "Quantum Electronics", Third Edition, John Wiley and Sons, Inc., New York, 1989.

M. G. Xu, J.-L. Archambault,L. Reekie and J. P. Dakin, "Discrimination between strain and temperature effects using dual-wavelength fibre grating sensors", *Elect. Lett.*, Vol. 30, No. 13, pp. 1085-1087, June 1994.

APPENDIX A

DERIVATION OF THE FIRST ORDER CORRECTION

A first order correction in $1/\alpha$ can be derived from the coupled mode equations of an optical fiber with a single Bragg grating. The procedure outlined here can also be applied to optical fibers with multiple Bragg gratings so correction terms in $1/\gamma_j$, j=2, 3, ..., can be obtained.

The method used to derive the first order correction is the so-called Piccard Method, also known as the Method of the Successive Approximation. This is a well known technique that can be used to obtain analytical approximated solutions to a system of differential equations after a certain number of iterations [Ince, 1956; Greenspan, 1960 and Rowe, 1962]. Basically it states that the sequence of solutions $\{c_{0,n}^{(+)}, c_{0,n}^{(-)}\}$, $n = 1, 2, \ldots$, of the system of differential equations

$$\frac{dc_{0,n}^{(+)}}{dZ} = -\frac{C_{00}\, i}{2}\left[\left(e^{\alpha i Z} + e^{\gamma i Z}\right) c_{0,n-1}^{(-)} + \left(e^{-(\alpha-\gamma) i Z/2} + e^{(\alpha-\gamma) i Z/2}\right) c_{0,n-1}^{(+)}\right] \tag{79}$$

$$\frac{dc_{0,n}^{(-)}}{dZ} = \frac{C_{00}\, i}{2}\left[\left(e^{-(\alpha-\gamma) i Z/2} + e^{(\alpha-\gamma) i Z/2}\right) c_{0,n-1}^{(-)} + \left(e^{-\alpha i Z} + e^{-\gamma i Z}\right) c_{0,n-1}^{(+)}\right] \tag{80}$$

converges to Eqs. (15) and (16) as $n \Rightarrow \infty$. The closer the initial trial functions $c_{0,0}^{(+)}$ and $c_{0,0}^{(-)}$ are to the "exact" solution, the faster the above sequence

converges. Consequently, by choosing appropriate trial functions the sequence of solutions may converge after only a few iterations. Actually, it has been found that the result obtained with the very first iteration, or the first order correction, compared very well with the numerical result. As mentioned before, the trial functions can be chosen to be the asymptotic solution. By substituting Eqs. (22) and (23) into (79) and (80), integrating the resulting equation, expanding it in powers of $1/\alpha$ and keeping the first order term in $1/\alpha$, they reduce to

$$c_{0,1}^{(+)} = c_{0,0}^{(+)} - \frac{C_{00}}{2\alpha}\left\{4\,i\,c_{0,0}^{(+)}\sin\left[\frac{1}{2}(\alpha-\gamma)Z\right] + c_{0,0}^{(-)}\,e^{\alpha i Z}\right\} - c_1^{(+)} \tag{81}$$

and

$$c_{0,1}^{(-)} = c_{0,0}^{(-)} + \frac{C_{00}}{2\alpha}\left\{4\,i\,c_{0,0}^{(-)}\sin\left[\frac{1}{2}(\alpha-\gamma)Z\right] - c_{0,0}^{(+)}\,e^{-\alpha i Z}\right\} - c_1^{(-)} \quad . \tag{82}$$

The constants of integration on the right hand side of the above equations, can be obtained by applying the boundary conditions of the problem. Their derivation is straight forward and given by

$$c_1^{(+)} = -\frac{C_{00}^2\sin\left(\frac{\eta}{2}\right)}{2\alpha\left[\eta\,i\cos\left(\frac{\eta}{2}\right) - \gamma\sin\left(\frac{\eta}{2}\right)\right]} \tag{83}$$

and

$$c_1(\theta) = -\frac{\eta\ C_{00}\ e^{(\gamma-2\alpha)i/2}\ i}{2\alpha\left[\eta\ i\cos\left(\frac{\eta}{2}\right)-\gamma\sin\left(\frac{\eta}{2}\right)\right]} \quad . \tag{84}$$

The range of values that the above approximation applies will now be investigated.

APPENDIX B

INTERVAL OF CONVERGENCE OF THE FIRST ORDER APPROXIMATION

A careful analysis of the solution of Eqs. (79) and (80) was made in order to determine its interval of convergency. The analysis consisted of determining an appropriate series expansion of the integrals involved and the values of the parameters for which the series converge. Basically, the integral which has to be solved and analysed was the following

$$I_{1,\pm} = \int c_{0,0}^{(\pm)} e^{\pm a i Z} \, dZ \tag{85}$$

where a can be either α, γ or $\alpha-\gamma$.

When $a=-\gamma$, the integrals in Equation (85) have very simple solutions given by

$$\int c_{0,0}^{(+)} e^{-\gamma i Z} \, dZ = - \frac{2 i c_{0,0}^{(-)}}{C_{00}} \tag{86}$$

and

$$\int c_{0,0}^{(-)} e^{\gamma i Z} \, dZ = \frac{2 i c_{0,0}^{(+)}}{C_{00}} \quad . \tag{87}$$

These solutions correspond to the zeroth order correction of the field amplitudes, they are obtained using the relations in Eqs. (22) and (23) and are good for any values of C_{00} and γ.

On the other hand, the remaining integrals are more involved and can be obtained in two different ways; the most obvious and straight-forward way, would be to directly substitute the values of the forward and backward amplitudes of the fields directly into the integrand. However, it has been found that this procedure does not give any information about the parametric values for which the resulting integral converges. For this reason, a second approach was attempted which consists of the following:

first an integration by parts of the term $e^{\pm a\, i Z}\, d Z$ was performed or

$$\int c_{0,0}^{(\pm)}\, e^{\pm a\, i Z}\, dZ = -\frac{i\, c_{0,0}^{(\pm)}\, e^{\pm a\, i Z}}{\pm a} + \frac{i}{\pm a}\int e^{\pm a\, i Z}\, \frac{dc_{0,0}^{(\pm)}}{dZ}\, dZ \qquad .(88)$$

Then a substitution of Eqs. (20) and (21) was made leading to

$$\int c_{0,0}^{(+)}\, e^{\pm a\, i Z}\, dZ = -\frac{i\, c_{0,0}^{(+)}\, e^{\pm a\, i Z}}{\pm a} + \frac{C_{00}}{\pm 2a}\int c_{0,0}^{(-)}\, e^{(\gamma \pm a)\, i Z}\, dZ \qquad (89)$$

$$\int c_{0,0}^{(-)}\, e^{\pm a\, i Z}\, dZ = -\frac{i\, c_{0,0}^{(-)}\, e^{\pm a\, i Z}}{\pm a} - \frac{C_{00}}{\pm 2a}\int c_{0,0}^{(+)}\, e^{(-\gamma \pm a)\, i Z}\, dZ \qquad (90)$$

Next, this procedure was repeated for the remaining integrals several times. Using the inductive method, it can be easily realized that the integrals can be written as the following series:

$$\int c_{0,0}^{(+)} e^{\pm i a Z} dZ = -i\left[\frac{c_{0,0}^{(+)}}{\pm a} + \frac{C_{00}\, c_{0,0}^{(-)} e^{\gamma i Z}}{\pm 2(\gamma \pm a)\, a}\right] e^{\pm i a Z} \sum_{m=0}^{\infty} \frac{C_{00}^{2m} / 2^{2m} (-1)^m}{[\pm a(\gamma \pm a)]^m} \tag{91}$$

and

$$\int c_{0,0}^{(-)} e^{\pm i a Z} dZ = -i\left[\frac{c_{0,0}^{(-)}}{\pm a} + \frac{C_{00}\, c_{0,0}^{(+)} e^{-\gamma i Z}}{\pm 2(\gamma - (\pm a))\, a}\right] e^{\pm i a Z} \sum_{m=0}^{\infty} \frac{C_{00}^{2m} / 2^{2m}}{[\pm a(\gamma - (\pm a))]^m} \tag{92}$$

The condition of convergency can be obtained directly from Eqs. (91) and (92) or

$$\frac{C_{00}^2}{|(\gamma - \alpha)(3\gamma - \alpha)|} < 1 \tag{93}$$

$$\frac{C_{00}^2}{4|(\gamma - \alpha)|\alpha} < 1 \tag{94}$$

and

$$\frac{C_{00}^2}{|(\gamma^2 - \alpha^2)|} < 1 \tag{95}$$

where the corresponding values for a have been substituted.

In conclusion, there are three different conditions of convergency for the integrals on the left hand side of Eqs. (89) and (90). Among those three conditions, the most restrictive one must be chosen. It must be emphasized that these conditions are necessary *but are not sufficient* for the series to converge. A necessary and sufficient condition would be achieved only after exhaustive analysis of the higher order approximations of the coupled mode differential equations, Eqs. (79) and (80), for n=2, 3, etc.

APPENDIX C

TYPICAL VALUES OF THE FIBER PARAMETERS

An examination of the typical values of the optical fiber Bragg grating parameters have been undertaken in order to determine their range of values. The parameters in question are α, the normalized phase matching parameter γ and the normalized coupling constant C_{00}. The results obtained are specifically for a fiber with a single Bragg grating however their order of magnitude values also apply to an optical fiber with two Bragg gratings.

The three parameters mentioned above are given by Eqs. (12) through (14). Nearby the phase matching condition γ is almost zero. This yields to a modulation frequency Ω given by

$$\Omega \cong 2\beta_0 \tag{96}$$

and

$$\alpha \cong 4\beta_0 L \cdot \tag{97}$$

The normalized coupling constant is given by Eqs. (8) and (14). Substituting the values of the electric field for a single mode fiber [Marcuse, 1973] and using the eigenvalue equation of a weakly guiding fiber to eliminate the Bessel functions J_1 and J_0 in favor of the modified Bessel functions K_1 and K_0, the normalized coupling constant reduces to

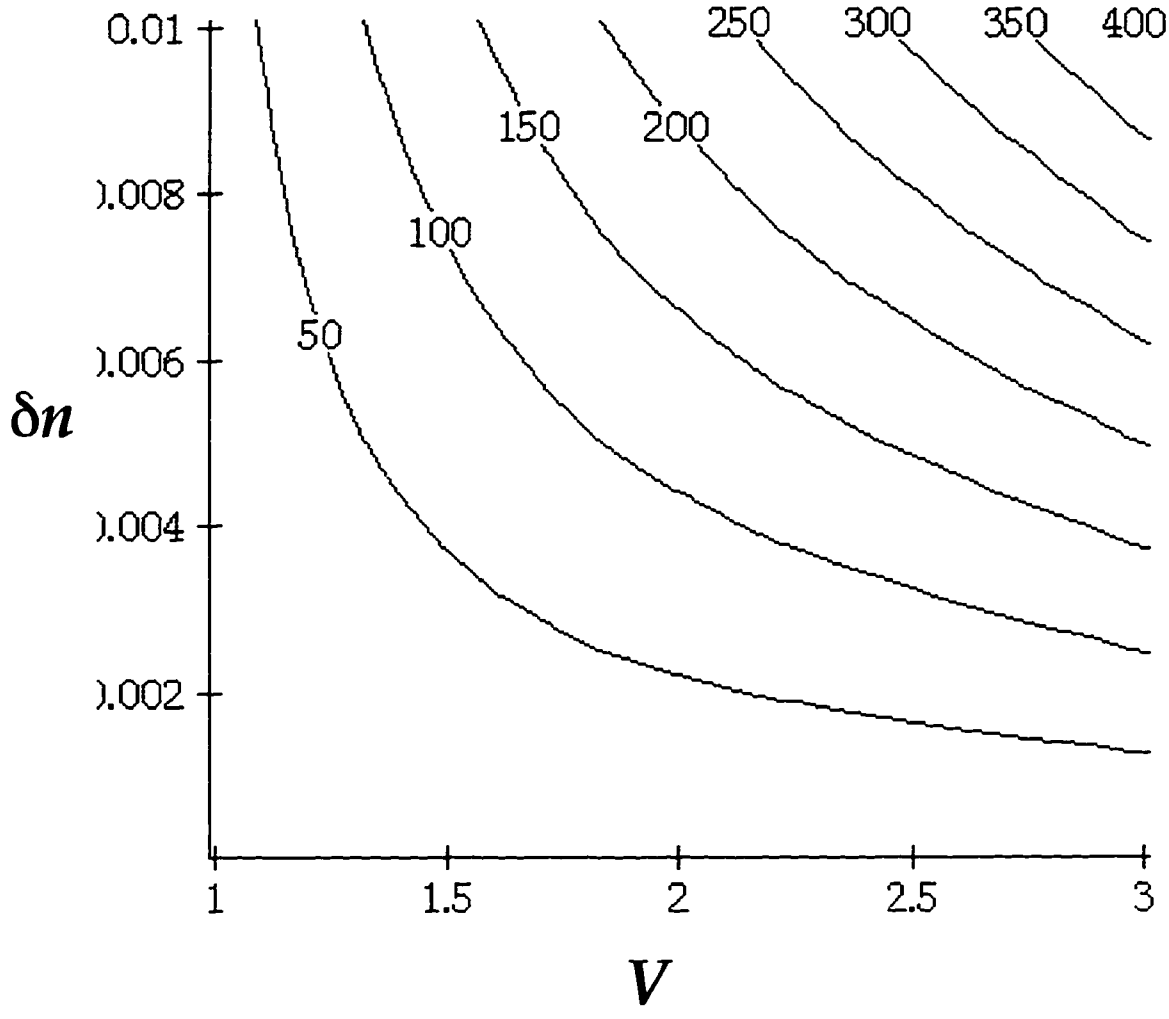

Figure 18. Contour plot of the normalized coupling constant against the V-number and the amplitude modulation of the refractive index for L=0.01m, n_{core}=1.46, a=5.0 μm, Δ=0.01.

$$C_{00} = \frac{2 L W^2 k^2 \delta n n_{core}}{\beta_0 V^2} \left\{ 1 + \left[\frac{U K_0(W)}{W K_1(W)} \right]^2 \right\} \quad . \qquad (98)$$

Equations (97) and (98) can now be plotted using the approximation for the eigenvalue W given by Marcuse [1974 and 1982] (see Figs. 18 and 19)

$$W = 1.122 \exp \left[- \frac{(\Delta + 1) J_0(V)}{V J_1(V)} \right] \quad . \qquad (99)$$

Typical values of the parameters involved are shown in the Figures. As it can be seen, the normalized coupling constant is anywhere between 0 and 400 whereas α can be as low as 50,000 and as high as 170,000.

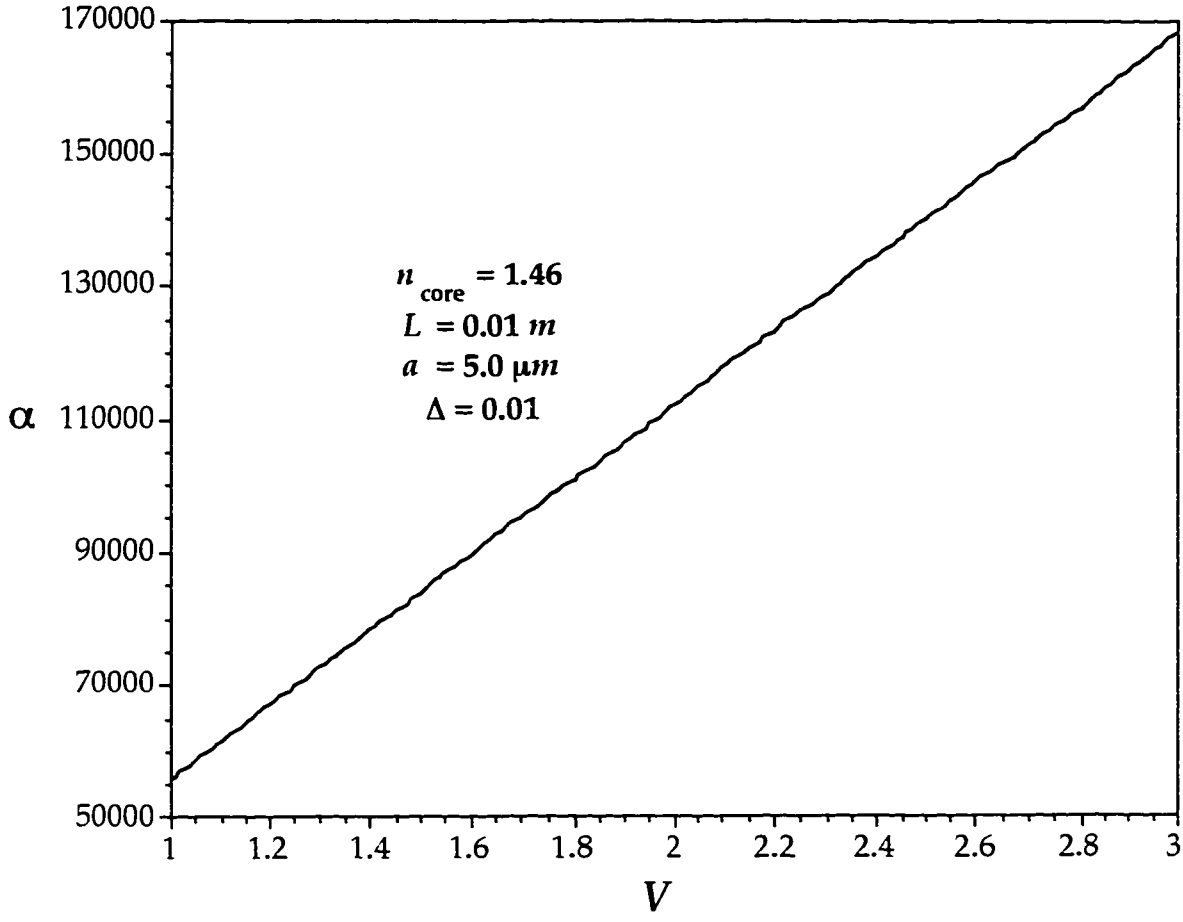

Figure 19. Plot of the α parameter against the V-number for L=0.01m, n_{core}=1.46, a=5.0 μm, Δ=0.01.

APPENDIX D

SOLUTION OF THE COUPLED EQUATIONS FOR TWO CO-PROPAGATING MODES

Using the procedure described in the previous appendices, results obtained with this work was compared with [Snyder and Davis, [1970]. In this case, the coupling was assumed to be between two co-propagating modes, i.e., the coupling between the forward and backward propagating modes was neglected. A negligible coupling between other modes is achieved whenever the frequency of modulation of the grating is tuned to match the difference between the propagation constant of two specific modes or

$$\Omega \cong \beta_0 - \beta_1 \tag{100}$$

where β_0 and β_1 are the propagation constant of the first and second modes, respectively. In the case where the first and second modes are the forward and backward fundamental modes, respectively, $\beta_1 = -\beta_0$ and the tunning condition must be $\Omega \cong 2\beta_0$.

When the above condition applies, coupling between the remaining modes is virtually suppressed. Deriving the asymptotic solution for two co-propagating modes using the Initial Conditions

$$c_0^{(+)}(Z=0) = 1 \quad \text{and} \quad c_1^{(+)}(Z=0) = 0$$

and applying a first order correction using the Piccard's method, it is obtained

$$c^{(+)}_{0,1} = c^{(+)}_{0,0} + \frac{\left[(\alpha' + 2\gamma')\, i\, c^{(+)}_{1,0} - c^{(+)}_{0,0}\, e^{i\gamma'\theta}\right]}{b_1 b_0 e^{-(\alpha'+\gamma')i\theta}} + c_{10} \tag{101}$$

and

$$c^{(+)}_{1,1} = c^{(+)}_{1,0} - \frac{\left[(\alpha' + 2\gamma')\, i\, c^{(+)}_{0,0} - c^{(+)}_{1,0}\, e^{-i\gamma'\theta}\right]}{b_1 b_0 e^{(\alpha'+\gamma')i\theta}} + c_{11} \tag{102}$$

where

$$c^{(+)}_{0,0} = \left[\cos(\eta'\theta) + \frac{\gamma\, i \sin(\eta'\theta)}{2\eta'}\right] e^{-\gamma' i\theta/2}\ , \tag{103}$$

$$c^{(+)}_{1,0} = \frac{e^{\gamma' i\theta/2} \sin(\eta'\theta)}{\eta'}, \tag{104}$$

$$c_{11} = \frac{(\alpha' + 2\gamma')\, i}{b_1 b_0}\ ,\ c_{10} = \frac{1}{b_1 b_0}\ , \tag{105}$$

$$\eta' = \frac{\sqrt{\gamma'^2 + 4}}{2} \tag{106}$$

and

$$b_1 b_0 = \left[\, 1 - (\alpha' + 2\gamma')(\alpha' + \gamma')\,\right]\ . \tag{107}$$

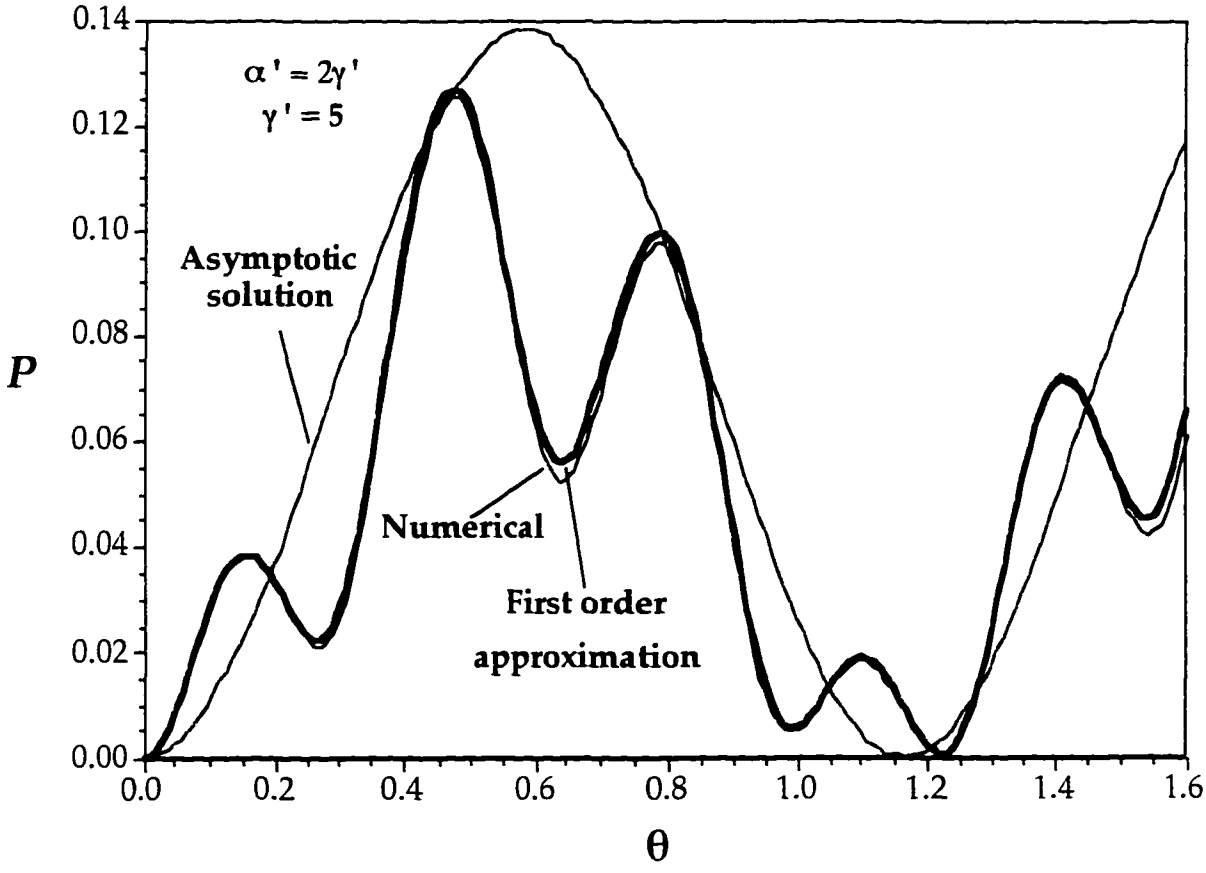

Figure 20. Comparison between the asymptotic, first order and numerical solutions for the transferred power against the normalized length of two co-propagating modes ($\alpha'=2\gamma'$, $\gamma'=5$).

In Eqs. (101) through (104), $c_{m,n}^{(+)}$ is the n^{th} order correction of the amplitude of the m^{th} forward propagating mode. Furthermore, the above parameters have been redefined to agree with Snyder and Davis notation or

$$\theta = \frac{Cz}{2} , \tag{108}$$

$$\gamma' = \frac{\Omega - \Delta\beta}{C/2}, \tag{109}$$

$$\alpha' = \frac{4\,\Delta\beta}{C} \tag{110}$$

$$\Delta\beta = \beta_1 - \beta_0 \tag{111}$$

where C is the coupling constant between the two modes.

A comparison between the transferred power obtained by Snyder and Davis, the power derived from Eq. (102) and the power using the numerical is shown in Figs. 20 through 23. As it can be seen, the first order solution in Figures 20 and 22 is very close to the numerical solution. For the higher value of α' (Figure 20), it is almost indistinguishable from the numerical result whereas for lower α' value it deviates slightly from the "exact" solution. Since the trial solution used was the asymptotic, it is expected that the first order correction works better in the interval of higher α' values.

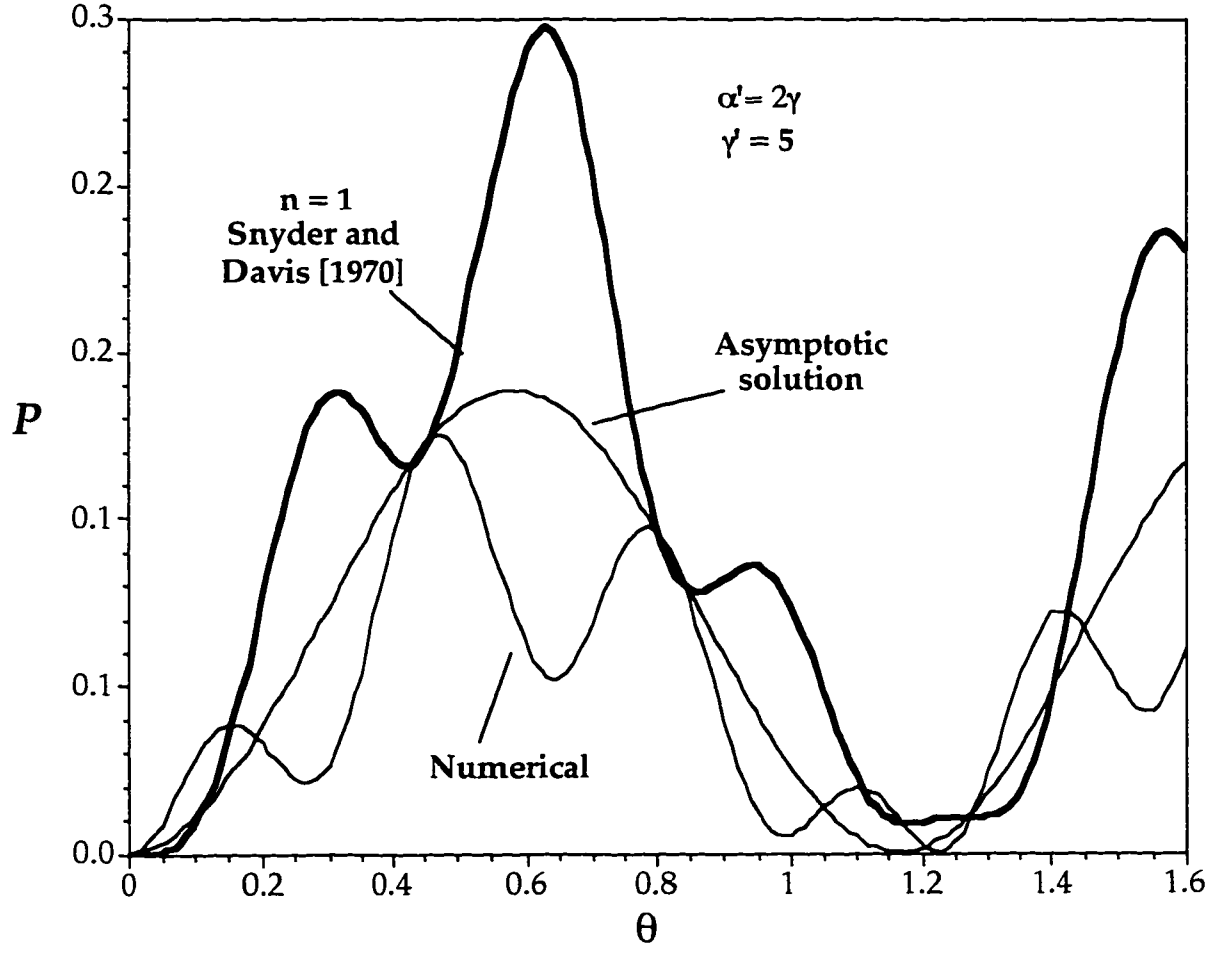

Figure 21. Comparison between the asymptotic, numerical and first order solutions of Snyder and Davis [1970] for the transferred power against the normalized length of two co-propagating modes ($\alpha'=2\gamma'$, $\gamma'=5$).

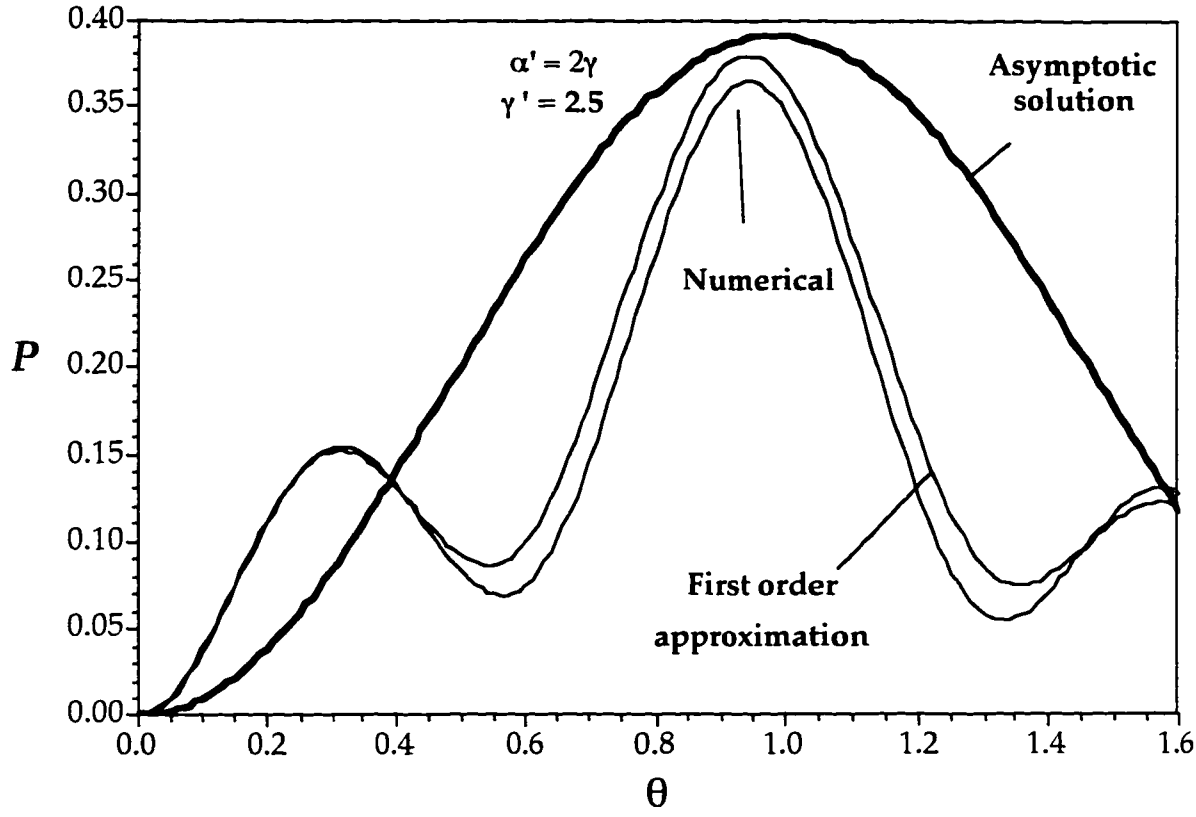

Figure 22. Comparison between the asymptotic, first order and numerical solutions for the transferred power against the normalized length of two co-propagating modes ($\alpha'=2\gamma'$, $\gamma'=2.5$).

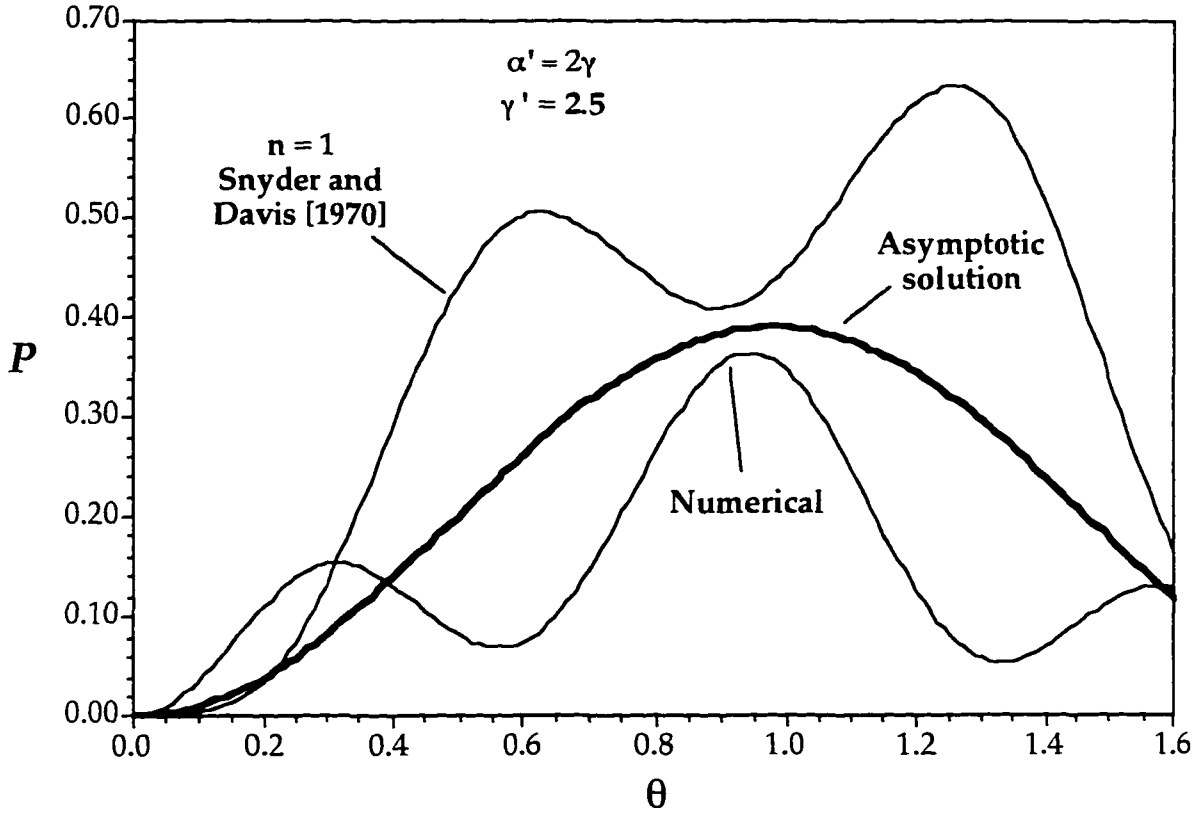

Figure 23. Comparison between the asymptotic, numerical and first order solutions of Snyder and Davis [1970] for the transferred power against the normalized length of two co-propagating modes ($\alpha'=2\gamma'$, $\gamma'=5$).

Additional comparisons were made between the numerical result and the first order approximations obtained by Equation (13) of Snyder and Davis [1970] (see Figures 21 and 23). Notice this first order approximation deviates by more than 100% from the numerical solution in several regions of the plot. This result is even worse than the asymptotic solution itself. In addition, it is important to point out that Snyder and Davis [1970] have obtained a different numerical result much closer to their approximation (see for instance, Figure 1 of Snyder and Davis [1970]). It is not known why their numerical result is so different from the one obtained. However, it is believed that their approximate solution does not yield an accurate result because of the lack of consistency of the method used. In their work it was initially assumed that the amplitudes of the modes could be expressed in terms of a series expansion of $1/\alpha'$ where the terms multiplied by the power would be *independent* of α', or

$$c_0^{(+)} = \sum_{n=0}^{\infty} \frac{c_{0,n}^{(+)}}{\alpha'^{\,n}} \tag{112}$$

and

$$c_1^{(+)} = \sum_{n=0}^{\infty} \frac{c_{1,n}^{(+)}}{\alpha'^{\,n}} \tag{113}$$

Accordingly $c_{0n}^{(+)}$ and $c_{1n}^{(+)}$ were assumed to be *independent* of α'. However, after some manipulations Snyder and Davis arrived at a result contrary to the initial assumption or

$$c^{(+)}_{0,1} = \frac{\alpha' c^{(+)}_{1,0}}{i(\gamma' + \alpha')} e^{i(\alpha' + \gamma')\theta} \tag{114}$$

and

$$c^{(+)}_{1,1} = \frac{\alpha'}{i(\gamma' + \alpha')}\left(c^{(+)}_{0,0} e^{-i(\alpha' + \gamma')\theta} - 1\right) \quad . \tag{115}$$

As it can be seen, Eqs. (114) and (115) -which correspond to Eqs. (12a) and (12b) of Snyder and Davis [1970] -, are not consistent with the initial assumption. This lack of consistency might have been the source of inaccuracy of their approximation.

VITA

Claudio Oliveira Egalon

Address: 2658 N. Armistead Ave. Apt. B-2, Hampton, VA, 23666, USA

Education: Ph.D. in Physics, The College of William and Mary, Williamsburg, VA., 1990.

M.Sc. in Physics, The College of William and Mary, 1988.

B.Sc. in Physics, Federal University of Rio de Janeiro, Rio de Janeiro, RJ, Brazil.

Dr. Egalon is currently a Senior Research Scientist for Analytical Services and Materials, Inc., working under contract for NASA Langley Research Center. He became the first Brazilian to conduct low gravity flight experiments in NASA's KC-135 aircraft in March 1993 and has conducted more than 290 low gravity parabolas. He is fluent in English, Spanish and Portuguese and holds a Private Pilot and Instrument Rate certificate. He has five patents awarded, twelve patents pending, thirty eight technical publications and has received nineteen NASA awards and certificates of recognition. He has biographical citations in "Who is Who in Science and Engineering", "Who is Who in America" and "Who is Who in the South and Southwest". His main research interests are optical fiber sensors and microgravity research.